Title: Osteopontin and iCD8α cells promote intestinal intraepithelial lymphocyte homeostasis

Running title: Osteopontin, iCD8α cells and intraepithelial lymphocytes

Authors: Ali Nazmi[*1], Michael J. Greer[†1], Kristen L. Hoek[*1], M. Blanca Piazuelo[‡], Joern-Hendrik Weitkamp[§], and Danyvid Olivares-Villagómez[*,¶]

[*]Department of Pathology, Microbiology and Immunology, Vanderbilt University Medical Center, A5301 Medical Center North, Nashville, Tennessee 37232, USA; [†]Department of Biomedical Informatics, Vanderbilt University, Nashville, Tennessee, 37232, USA; [‡]Department of Medicine, Vanderbilt University Medical Center, 1030 MRBIV, Nashville, Tennessee 37232, USA; [§]Department of Pediatrics, Vanderbilt University Medical Center, Monroe Carell Jr. Children's Hospital, 111114 Doctor's Office Tower, Nashville, Tennessee 37232, USA; [¶]Vanderbilt Institute for Infection, Immunology and Inflammation, Vanderbilt University Medical Center, A5301 Medical Center North, Nashville, Tennessee 37232, USA.

Corresponding author: Danyvid Olivares-Villagómez, Department of Pathology, Microbiology and Immunology, Vanderbilt University Medical Center, A5301 Medical Center North, Nashville, Tennessee 37232, USA. Telephone, 615-936-0134. Fax, 615-343-7392. Email, danyvid.olivares-villagomez@vumc.org. ORCID, 0000-0002-1158-8976.

[1]These authors contributed equally to this report

This work was supported by NIH grant R01DK111671 (D.O-V.); Careers in Immunology Fellowship Program from the American Association of Immunologists (D.O-V. and A.N.); National Library of Medicine T15 LM00745 grant (M.J.G); scholarships from the Digestive

24 Disease Research Center at Vanderbilt University Medical Center supported by NIH gran
25 P30DK058404; and the Vanderbilt Genome Editing Resource supported by a Diabetes Research
26 and Training Center Grant (DK020593) and Cancer Center Support Grant (CA68485)

Abstract

Intestinal intraepithelial lymphocytes (IEL) comprise a diverse population of cells residing in the epithelium at the interface between the intestinal lumen and the sterile environment of the lamina propria. Because of this anatomical location, IEL are considered critical components of intestinal immune responses. Indeed, IEL are involved in many different immunological processes ranging from pathogen control to tissue stability. However, despite their critical importance in mucosal immune responses, very little is known about the homeostasis of different IEL subpopulations. The phosphoprotein osteopontin is important for critical physiological processes, including cellular immune responses such as survival of Th17 cells and homeostasis of NK cells, among others. Because of its impact in the immune system, we investigated the role of osteopontin in the homeostasis of IEL. Here, we report that mice deficient in the expression of osteopontin exhibit reduced numbers of the IEL subpopulations TCR$\gamma\delta^+$, TCRβ^+CD4$^+$, TCRβ^+CD4$^+$CD8α^+ and TCRβ^+CD8$\alpha\alpha^+$ cells in comparison to wild-type mice. For some IEL subpopulations the decrease in cells numbers could be attributed to apoptosis and reduced cell division. Moreover, we show *in vitro* that exogenous osteopontin stimulates the survival of murine IEL subpopulations and unfractionated IEL derived from human intestines, an effect mediated by CD44, a known osteopontin receptor. We also show that iCD8α IEL, but not TCR$\gamma\delta^+$ IEL, TCRβ^+ IEL or intestinal epithelial cells, can promote survival of different IEL populations via osteopontin, indicating an important role for iCD8α cells in the homeostasis of IEL.

Key Points

1. Osteopontin promotes homeostasis of mouse and human IEL, mediated by its ligand CD44
2. iCD8α cells produce osteopontin which impacts the survival of other IEL
3. Lack of osteopontin renders mice susceptible to intestinal inflammation

50 **Introduction**

51 One of the largest immunological compartments in the body is comprised of intraepithelial
52 lymphocytes (IEL), a group of immune cells interspaced between the monolayer of intestinal
53 epithelial cells (IEC). IEL can be divided into two groups based on T cell receptor (TCR)
54 expression (1-3). TCR^+ IEL express αβ or γδ chains. $TCR\alpha\beta^+$ IEL can be further subdivided into
55 $TCR\alpha\beta^+CD4^+$, $TCR\alpha\beta^+CD4^+CD8\alpha\alpha^+$, $TCR\alpha\beta^+CD8\alpha\alpha^+$, and $TCR\alpha\beta^+CD8\alpha\beta^+$ cells. TCR^{neg}
56 IEL comprise innate lymphoid cells (ILC) (4-6) and lymphocytes characterized by expression of
57 intracellular CD3γ chains ($iCD3^+$), some of which express CD8αα (iCD8α cells) (7, 8).

58 Because of their anatomical location, IEL function as sentinels between the antigenic
59 contents of the intestinal lumen and the sterile environment under the basal membrane of the
60 epithelium. Indeed, TCRγδ IEL surveil for pathogens (9), secrete antimicrobials conferring
61 protection against pathobionts (10), and protect from intestinal inflammation (11). Other IEL, like
62 conventional CD8 T cells that migrate into the epithelium, can protect against *Toxoplasma*
63 infection (12) and reside in this organ as memory cells (13, 14). $TCR\alpha\beta^+CD4^+CD8\alpha\alpha^+$ IEL can
64 prevent development of disease in the T cell adoptive transfer model of colitis (15). iCD8α cells
65 confer protection against *Citrobacter rodentium* infection and may protect against necrotizing
66 enterocolitis in neonates (8), but these cells can also promote intestinal inflammation in some
67 experimental conditions (16). $iCD3^+$ IEL are involved in malignances associated with celiac
68 disease (7).

69 Osteopontin is a glycosylated phosphoprotein encoded by the Spp-1 (secreted
70 phosphoprotein) gene, originally characterized as part of the rat bone matrix (17, 18). Osteopontin
71 is a versatile molecule involved in many physiological and disease processes (19-21). The role of
72 osteopontin in intestinal inflammation is diverse. For example, Spp-1-deficient mice present with

73 milder disease in the trinitrobenzene sulphonic acid and DSS models of colitis (22, 23). In humans
74 with inflammatory bowel diseases (IBD), plasma osteopontin is significantly increased compared
75 to healthy individuals (24, 25). Some reports indicate that osteopontin is downregulated in the
76 mucosa of Crohn's disease (CD) patients (26), whereas other groups have reported higher
77 osteopontin expression in the intestines of individuals with CD and ulcerative colitis (UC)
78 compared with healthy controls (25, 27). Because of its involvement in IBD, this molecule could
79 be a potential biomarker (28) and has been explored as a therapeutic target in clinical trials (29).
80 These reports clearly underscore the importance of osteopontin in intestinal inflammation and
81 warrant further investigation of this molecule in mucosal immune responses.

82 Studies of osteopontin in the immune system have provided important insight into the role
83 of this molecule. For example, osteopontin is involved in macrophage chemotaxis (30), inhibition
84 of NK cell apoptosis and promotion of NK cell responses (31), as well as modulation of dendritic
85 cell function (32). In terms of T cells, osteopontin has been shown to stimulate the survival of
86 concanavalin A-activated lymph node T cells *in vitro*, to promote the survival of anti-myelin
87 specific T cells in the central nervous system (33), and to stimulate Th1 responses (34). However,
88 because IEL are different from "conventional" T cells, and have varied and distinct developmental
89 pathways and functions specialized for the environment of the intestinal epithelium (3), what has
90 been investigated for T cells in other anatomical compartments may not directly translate to IEL,
91 underscoring the need to investigate the role of osteopontin in this peculiar immune site. What we
92 know about the role of osteopontin and IEL homeostasis is very limited. For example, it was
93 reported that the frequency and numbers of TCR$\gamma\delta^+$ IEL were reduced in osteopontin-deficient
94 mice, while unfractionated TCR$\alpha\beta^+$ IEL numbers remained similar in comparison to wild type
95 controls (35). However, *in vitro* neutralization of IEL-derived osteopontin resulted in decreased

96 survival of TCRγδ and TCRαβ IEL (35), confounding the *in vivo* results. Our group has recently
97 shown that iCD8α IEL enhance the survival of ILC1-like IEL, via osteopontin, impacting the
98 development of intestinal inflammation (36). Here, we hypothesize that osteopontin and iCD8α
99 cells are key components involved in the homeostasis of most IEL populations. In the present
100 report, we investigated this hypothesis by carefully studying the role of osteopontin in the
101 homeostasis of different IEL subpopulations in mice and total IEL derived from human tissue. We
102 present data showing that osteopontin differentially influences the survival, proliferation and
103 migration of distinct IEL subpopulations, and that these effects are mediated in part by one of the
104 many osteopontin ligands, CD44. Furthermore, we show that IEL survival is mediated primarily
105 by iCD8α cell-derived osteopontin, whereas other TCRγδ$^+$ and TCRβ$^+$ IEL do not contribute, at
106 least *in vitro*, to the survival of IEL. Moreover, our *in vivo* experiments show that IEC-derived
107 osteopontin do not seem to promote IEL survival. Finally, we present evidence of the impact of
108 osteopontin in the development of intestinal inflammation.
109

110 **Material and methods**

111 *Mice*. C57BL/6J were originally purchased from The Jackson Laboratory (000664) and have been
112 maintained and acclimated in our colony for several years. CD44$^{-/-}$ (005085), CD45.1 (002014),
113 RFP-Foxp3 (008374) and Spp-1$^{-/-}$ (004936) mice on the C57BL/6 background were originally
114 purchased from The Jackson Laboratory. Rag-2$^{-/-}$ mice on the C57BL/6 background were provided
115 by Dr. Luc Van Kaer. Spp-1$^{-/-}$, CD44$^{-/-}$, and Rag-2$^{-/-}$ mice were crossed with C57BL/6J wild-type
116 mice to generate heterozygous offspring, and subsequently bred among themselves to generate
117 mutant mice. Vill-Cre$^{+/-}$ mice were provided by the laboratory of Dr. Keith Wilson. Spp-1$^{fl/fl}$ mice
118 in the C57BL/6J background were generated by the Vanderbilt Transgenic Mouse/ES Cell Shared
119 Resource following an established protocol (37). Briefly, intron 1/2 and intron 3/4 of the Spp-1
120 gene were targeted for insertion of LoxP sites by CRISPR/Cas9 ribonucleoproteins (RNP) along
121 with a 1528 bp megamer symmetrical donor ssDNA oligonucleotide (IDT). crRNA sequences
122 were 5'-GTGTGATAACACAGACTCAT-3' and 5'-AACCAGTACCTTACATGTT-3'. Vill-
123 Cre$^{+/-}$Spp-1$^{fl/fl}$ and Vill-Cre$^{-/-}$Spp-1$^{fl/fl}$ littermate mice were generated by crossing Vill-Cre$^{+/-}$ mice
124 and Spp-1$^{fl/fl}$ mice. Spp-1$^{-/-}$Rag-2$^{-/-}$ mice were generated in our colony by breeding Spp-1$^{+/-}$ with
125 Rag-2$^{+/-}$ mice. Male and female mice were used for all experiments. Mice were maintained in
126 accordance with the Institutional Animal Care and Use Committee at Vanderbilt University.

127

128 *Lymphocyte isolation*. IEL were isolated by mechanical disruption as previously reported (38).
129 Briefly, after flushing the intestinal contents with cold HBSS and removing excess mucus, the
130 intestines were cut into small pieces (~1 cm long) and shaken for 45 minutes at 37°C in HBSS
131 supplemented with 5% fetal bovine serum and 2 mM EDTA. Supernatants were recovered and
132 cells isolated using a discontinuous 40/70% Percoll (General Electric) gradient. To obtain lamina

133 propria lymphocytes, intestinal tissue was recovered and digested with collagenase (187.5 U/ml,
134 Sigma) and DNase I (0.6 U /ml, Sigma). Cells were isolated using a discontinuous 40/70% Percoll
135 gradient. Spleen cells were isolated by conventional methods.
136
137 *Human samples.* The Vanderbilt University Medical Center Institutional Review Board approved
138 sample collection (IRB# 090161 and 190182). Peripheral blood mononuclear cells were isolated
139 by ficoll gradient from unidentified healthy adult volunteers as previously described (39). A
140 pathologist from the Vanderbilt Children's Hospital provided de-identified fresh intestinal tissue
141 specimens from infants. Isolation of human cells associated with the intestinal epithelium was
142 performed as previously described (40). Briefly, tissue was cut in small ~1 cm pieces and incubated
143 with slow shaking for 30 minutes at room temperature in HBSS (without calcium and magnesium)
144 supplemented with 5% fetal bovine serum, 5mM EDTA and 1% antibiotic mix (pen-strep-
145 AmphoB; Fisher-Lonza). After incubation, cells in the supernatant were recovered.
146
147 *Reagents and flow cytometry.* Fluorochrome-coupled anti-mouse CD4 (GK1.5), -CD44 (1M7), -
148 CD45 (30F11), CD45.1 (A20), CD45.2 (104), -CD8α (53–6.7), -CD8β (REA793 or H35-17.2), -
149 TCRβ (H57-597), -TCRγδ (eBioGL3), Ki69 (solA15) and isotype controls were purchased from
150 Thermofisher, BD Biosciences or Tonbo. Annexin V and 7AAD were purchased from BD
151 Biosciences. All staining samples were acquired using BD FACS Canto II or 4-Laser Fortessa
152 Flow cytometers (BD Biosciences) and data was analyzed using FlowJo software (Tree Star). Cell
153 staining was performed following conventional techniques. Manufacturer's instructions were
154 followed for Annexin V staining; briefly, early apoptotic cells were considered as annexin
155 $V^{+}7AAD^{neg}$, late apoptotic cells or undergoing necrosis as annexin $V^{+}7AAD^{+}$, and necrotic cells

156 as annexin V^-7AAD^+. FACS sorting was performed using a FACSAria III at the Flow Cytometry
157 Shared Resource at VUMC.
158
159 *In vitro survival assay.* FACS-enriched IEL subpopulations were incubated in a 96-well flat-
160 bottom well plate (Falcon, Fisher Scientific) at a density of $5x10^5$ cells/ml in RPMI containing
161 10% fetal bovine serum. In some groups culture media was supplemented with recombinant
162 osteopontin (2 μg/ml) (R&D) or anti-CD44 (5 μg/ml) (Thermofisher; clone IM7). Cells were
163 cultured in 5% CO_2 at 37°C. At time 0 and every 24 h, an aliquot from the culture was taken to
164 count live cells using trypan blue to exclude dead cells. Percentage of live cells was calculated in
165 reference to time 0. For human samples, total PBMC or IEL were cultured in the presence or
166 absence of recombinant human osteopontin (2 μg/ml) (R&D) and anti-human-CD44 (5 μg/ml)
167 (Thermofisher; clone IM7).
168
169 *Co-culture survival assays.* $CD45^+$ IEL from Spp-$1^{-/-}$ mice were positively selected using magnetic
170 beads (Miltenyi) and cultured ($1x10^5$ cells/well) in a 96-well flat-bottomed well plate in RPMI
171 complemented with 10% fetal bovine serum, penicillin/streptomycin, HEPES, L-glutamine and β-
172 mercaptoethanol. These are "read out" cells. Then, these cells were cultured in the presence ($1x10^5$
173 cells/well) or absence of magnetic bead-enriched (Miltenyi) iCD8α cells from Rag-$2^{-/-}$ mice, or
174 $TCR\beta^+$ or $TCR\gamma\delta^+$ IEL from CD45.1 WT mice. For normalization purposes, the purity of these
175 cells was determined by flow cytometry. Anti-osteopontin antibodies (2 μg/ml) (R&D; clone
176 AF808) were added to some wells. After 4 h of incubation, cells were recovered and stained for
177 surface markers, 7AAD and Annexin V. For all experiments, IEL were gated according to their
178 size in a forward versus side scatter. Then, cells were selected by their expression of CD45.2 and

179 gated for the individual subpopulations, followed by analysis of 7AAD incorporation and annexin
180 V staining. Increased survival was determined as 100 - [% of annexin V^+ read-out cells in co-
181 culture x 100 / % of annexin V^+ cells cultured alone]. Osteopontin concentration from these
182 cultures was determined by an ELISA kit (R&D) following the manufacturer's instructions.
183
184 *Adoptive transfer of total T cells*. Total splenocytes from WT mice were depleted of CD19-positive
185 cells using magnetic beads (Miltenyi). Four to 6 million cells were adoptively transferred (i.p.)
186 into Rag-$2^{-/-}$ or Spp-$1^{-/-}$Rag-$2^{-/-}$ mice (similar results were observed regardless of the number of
187 cells transferred). Starting weight was determined prior to injection. Seven or 28 days later,
188 recipient mice were weighed, sacrificed and donor cells from the intestines analyzed by flow
189 cytometry. In some experiments a segment of the colon was excised and prepared for histological
190 examination. In some experiments CD19-depleted splenocytes from $CD44^{-/-}$ mice were adoptively
191 transferred into Rag-$2^{-/-}$ or Spp-$1^{-/-}$Rag-$2^{-/-}$ mice. Mice were weighed weekly for 4 weeks, and cells
192 and colon analyzed as indicated above. Pathological evaluation of the colons was done in a blind
193 fashion by Dr. Piazuelo, following established parameters (41).
194
195 *In vitro and in vivo Foxp3 expression*. Lamina propria lymphocytes isolated from RFP-Foxp3 mice
196 were cultured in the presence or absence of recombinant osteopontin and anti-CD44 antibodies as
197 described above. At time 0 and 72 h later, cells were analyzed by flow cytometry to detect RFP
198 expression in live TCR^+CD4^+ cells. For *in vivo* experiments, $CD4^+RFP^+$ splenocytes were enriched
199 by FACS and 2 x 10^5 cells were adoptively transferred i.p. into Rag-$2^{-/-}$ or Spp-$1^{-/-}$Rag-$2^{-/-}$ mice.
200 Eight weeks later, IEL were isolated and RFP expression analyzed in $CD45^+TCR\beta^+CD4^+$ donor-
201 derived cells.

202

203 *Transcription profile analysis.* For gene expression array, RNA was isolated from FACS-enriched
204 IEL subpopulations from 4 individual WT and Spp-1$^{-/-}$ mice. Samples were prepared for RT^2
205 Profiler PCR Array (QIAGEN PAMM-012Z) and analyzed following manufacturer's instructions.
206 For RNAseq analysis, RNA was isolated from FACS-enriched CD45$^+$ IEL derived from WT mice
207 cultured for 24 h in the presence or absence of recombinant osteopontin using the QIAGEN
208 RNeasy micro kit. Sequencing was performed on an Illumina NovaSeq 6000 (2 x 150 base pair,
209 paired-end reads). The tool Salmon (42) was used for quantifying the expression of RNA
210 transcripts. The R project software along with the edgeR method (43) was used for differential
211 expression analysis. For gene set enrichment analysis (GSEA), RNAseq data was ranked according
212 to the t-test statistic. The gene sets curated (C2), GO (C5), immunological signature collection
213 (C7) and hallmarks of cancer (H) of the Molecular Signatures Database (MSigDB) were used for
214 enrichment analysis. GSEA enrichment plots were generated using the GSEA software (44) from
215 the Broad Institute with 1000 permutations.

216

217 *Real time PCR for osteopontin expression*. RNA from colon tissue was isolated using Trizol
218 following the manufacturer's instructions. First strand cDNA was synthesized using RT2 first
219 strand kit (Qiagen). Real time PCR was performed using RT2 SYBR Green Mastermix (Qiagen).
220 Osteopontin and GADPH primers were from Qiagen.

221

222 *Statistical analysis.* Statistical significance between 2 groups was determined using Mann-
223 Whitney U-test. For analysis of 3 groups or more, two-way ANOVA followed by Dunn's multiple

224 comparison tests were used appropriately. All data was analyzed in GraphPad Prism 7 and shown

225 as mean ± standard error mean (SEM). A P value <0.05 was considered significant.

226

227

228 **Results**

229 *Osteopontin deficiency has a differential effect on the homeostasis of individual IEL populations*

230 A previous report has shown that mice deficient in osteopontin (Spp-1$^{-/-}$) have reduced TCRγδ^{+}
231 total cell numbers in the small intestine, while unfractionated TCRαβ^{+} IEL numbers remained the
232 same (35). In the same report, *in vitro* experiments showed that the survival of both of these IEL
233 populations was decreased when cultured in the presence of anti-osteopontin antibodies (35). To
234 further investigate, we analyzed in detail the IEL compartment of WT and Spp-1$^{-/-}$ mice. Fig. 1A
235 depicts the gating strategy used. Our analysis showed a decrease in TCRγδ^{+} small intestine IEL,
236 but contrary to the report by Ito et al (35), we observed that Spp-1$^{-/-}$ mice presented significant
237 reduction in the total numbers of total TCRβ^{+} cells and IEL subpopulations TCRβ^{+}CD4^{+},
238 TCRβ^{+}CD8α^{+} (which includes CD8αβ^{+} and CD8αα^{+}), and TCRβ^{+}CD4^{+}CD8α^{+} in comparison to
239 cells derived from WT mice (Fig. 1B, top rows). IEL deficiencies were also observed in the colons
240 of Spp-1$^{-/-}$ mice (Fig. 1B bottom rows). TCR^{neg} and iCD8α IEL, presented similar total cell
241 numbers in the small intestine of Spp-1$^{-/-}$ and WT mice but reduced numbers in the colons of Spp-
242 1$^{-/-}$ mice (Fig. 1B). Further subdivision of TCRβ^{+}CD8α^{+} IEL based on CD8β expression, showed
243 reduction in small intestine TCRβ^{+}CD8αα^{+} and TCRβ^{+}CD8αβ^{+} IEL numbers in Spp-1$^{-/-}$ mice
244 (Supplemental Fig. 1A and 1B). In the colon, while the number of TCRβCD8αβ^{+} IEL were similar
245 between WT and Spp-1$^{-/-}$ mice, there was a significant reduction in the total cell numbers of
246 TCRβ^{+}CD8αα^{+} IEL in Spp-1$^{-/-}$ mice (Supplemental Fig. 1A and 1B). Interestingly, osteopontin
247 deficiency did not affect spleen T lymphocytes (Fig. 1C) or lamina propria CD19^{+}, TCRβ^{+}CD4^{+},
248 and TCRβ^{+}CD8^{+} cells (Fig. 1D), suggesting that the major influence of this molecule is confined
249 to the intestinal IEL compartment.

250 To investigate whether the reduction in IEL numbers in Spp-1$^{-/-}$ mice was due to increased
251 cell death, we stained the cells with annexin V and 7AAD to determine the levels of early apoptosis
252 (annexin V^{+}7AAD^{neg}), late apoptosis/undergoing necrosis (annexin V^{+}7AAD^{+}) and necrosis
253 (annexin V^{-}7AAD^{+}). TCRγδ^{+}, TCRβ^{+}CD4^{+}, TCRβ^{+}CD4^{+}CD8α^{+}, TCRβ^{+}CD8αα^{+}, and
254 TCRβ^{+}CD8αβ^{+} IEL derived from Spp-1$^{-/-}$ and WT mice presented similar levels of cells in early
255 apoptosis (annexin V^{+}7AAD^{neg}) and necrosis (annexin V^{neg}7AAD^{+}) (Fig. 2A). On the other hand,
256 TCRγδ^{+}, TCRβ^{+}CD4^{+}, and TCRβ^{+}CD4^{+}CD8α^{+} IEL derived from Spp-1$^{-/-}$ mice presented an
257 increase in cells in late apoptosis/undergoing necrosis (annexin V^{+}7AAD^{+}), suggesting that the
258 decreased total numbers of these IEL subpopulations in the absence of osteopontin may be due to
259 increased cell death.

260 We also analyzed the cell division potential of TCRγδ^{+}, TCRβ^{+}CD4^{+}, TCRβ^{+}CD4^{+}CD8α^{+}
261 and TCRβ^{+}CD8αα^{+} and TCRβ^{+}CD8αβ^{+} IEL derived from WT and Spp-1$^{-/-}$ mice. TCRβ^{+}CD4^{+},
262 TCRβ^{+}CD4^{+}CD8α^{+} and TCRβ^{+}CD8αα^{+} IEL from osteopontin-deficient mice presented
263 decreased Ki67 staining in comparison to IEL derived from WT mice (Fig. 2B), indicating lower
264 proliferation of these IEL populations. Interestingly, TCRγδ^{+} IEL had similar Ki67 staining levels
265 in cells from osteopontin-deficient and -competent mice (Fig. 2B).

266 Overall, these results show that osteopontin is required for proper IEL cell numbers,
267 survival and cell division. Importantly, the effect caused by osteopontin is not homogeneous across
268 most IEL populations, and instead, each IEL population responds differently to this cytokine.

269

270 *IEL subpopulations survive better* in vitro *in the presence of osteopontin*

271 To investigate the role of osteopontin in IEL survival, we cultured FACS-enriched TCRγδ^{+},
272 TCRβ^{+}CD4^{+}, TCRβ^{+}CD8α^{+}, and TCRβ^{+}CD4^{+}CD8α^{+} IEL subpopulations in the presence or

273 absence of recombinant osteopontin, and measured survival every 24 h for a period of 3 days.
274 More than 50% of TCR$\gamma\delta^+$ IEL died after only 24 h of incubation with plain media and continued
275 to die after 48 and 72 h (Fig. 3A). Although TCR$\gamma\delta^+$ IEL incubated in the presence of osteopontin
276 showed cell death during the first 48 h of cultures, their survival at 72 h was higher than cells
277 incubated without recombinant osteopontin (Fig. 3A). A similar increased survival trend was
278 observed for TCRβ^+CD8α^+ and TCRβ^+CD4$^+$CD8α^+ IEL (Fig. 3A). TCRβ^+CD4$^+$ IEL were more
279 viable than the other populations at 24 h post culture even without recombinant osteopontin, but
280 addition of this cytokine maintained a constant survival rate of TCRβ^+CD4$^+$ IEL (Fig. 3A).
281 Osteopontin binds to several integrin receptors including αvβ1, αvβ3, and αvβ5, among others
282 (45), but also interacts with CD44 (46). Staining TCR$\gamma\delta^+$ and unfractionated TCRβ^+ IEL from
283 naïve mice with CD44 results in ~40 to 50% CD44$^+$ cells respectively (Supplemental Fig. 1C). To
284 determine whether the improved survival observed in the presence of osteopontin depends on
285 CD44 binding, IEL subpopulations were incubated in the presence of recombinant osteopontin and
286 anti-CD44 antibody. As shown in Fig. 3A, whenever IEL survival was improved by osteopontin,
287 this effect was blunted by addition of anti-CD44.

288 To determine whether osteopontin-mediated survival is specific for IEL, we investigated
289 the influence of osteopontin on the survival of splenic T cells. First, CD45$^+$ splenocytes from naïve
290 WT mice were cultured in the presence or absence of recombinant osteopontin. As shown in Fig.
291 3B, survival of CD45$^+$ spleenocytes was not affected by osteopontin. Moreover, FACS-enriched
292 TCRβ^+CD44^{hi} spleen cells from naïve WT and Spp-1$^{-/-}$ mice cultured in the presence or absence
293 of recombinant osteopontin and/or anti-CD44 presented no difference in their survival (Fig. 3C),
294 indicating that osteopontin preferentially influences the *in vitro* survival of IEL via CD44 but not
295 of total or CD44$^+$ splenic T cells.

296 The immune system of mice maintained in specific pathogen-free conditions more closely
297 resembles that of human neonates rather than adults (47). Therefore, to determine whether our
298 findings with murine IEL are relevant to humans, we isolated total IEL from human neonates and
299 cultured them in the presence or absence of recombinant human osteopontin. Human IEL survived
300 better in the presence of recombinant osteopontin than in its absence, and the addition of anti-
301 human CD44 blunted the cytokine effect (Fig. 3D), in parallel to the results observed with mouse
302 IEL. To determine the effect of osteopontin on other human lymphocytes, we employed PBMC
303 from healthy adults, as we were unable to obtain PBMCs from the same neonate individuals for
304 this purpose. As shown in Fig. 3E, PBMC survival was not enhanced or reduced by any of the
305 treatments used, which corroborates an intestinal IEL-specific effect. Overall, our results indicate
306 that in *in vitro* conditions, osteopontin differentially promotes both murine and human IEL
307 survival, an effect that is blunted by blocking its interaction with CD44.
308 Because anti-CD44 blocked the survival effect mediated by osteopontin, we investigated
309 whether the IEL compartment is disrupted in CD44-deficient mice. In comparison to IEL derived
310 from WT mice, $CD44^{-/-}$ mice presented reduced TCR^{neg} and $TCR\beta^{+}CD4^{+}$ IEL in the small
311 intestines, whereas the colon presented reduction in unfractionated $TCR\beta^{+}$, TCR^{neg}, $TCR\beta^{+}CD4^{+}$,
312 and $TCR\beta^{+}CD8\alpha^{+}$ IEL (Supplementary Fig. 1D).
313
314 *Osteopontin induces a differential anti-apoptotic gene expression in IEL*
315 The previous sections suggest an important role for osteopontin in the survival of different IEL
316 subpopulations. To investigate whether osteopontin induces a survival gene expression profile, we
317 isolated RNA from FACS-enriched $TCR\gamma\delta^{+}$, $TCR\beta^{+}CD4^{+}$, $TCR\beta^{+}CD8\alpha^{+}$ and
318 $TCR\beta^{+}CD4^{+}CD8\alpha^{+}$ IEL derived from naïve WT and Spp-$1^{-/-}$ mice, and determined the expression

319 of genes involved in preventing apoptosis. Comparison of genes expressed in IEL from WT and
320 Spp-1$^{-/-}$ mice showed that TCR$\gamma\delta^+$ cells from WT animals had more differentially expressed anti-
321 apoptotic genes in comparison to the other IEL populations (Supplemental Fig. 2A and B).
322 TCRβ^+CD8α^+ IEL presented little differential expression among the anti-apoptotic genes
323 analyzed. On the other hand, TCRβ^+CD4$^+$ and TCRβ^+CD4$^+$CD8α^+ IEL differentially expressed
324 some of these genes (Supplemental Fig. 2A and B). Birc2, a known inhibitor of apoptosis in
325 malignancies (48), was one of the genes consistently differentially expressed in most IEL analyzed
326 from WT mice, including TCRβ^+CD4$^+$CD8α^+ cells (Supplemental Fig. 2A and B). Overall, these
327 results indicate that osteopontin induces the expression of anti-apoptotic genes, but the gene profile
328 varies between different IEL subpopulations.

329 Because addition of recombinant osteopontin rescued IEL survival when cultured *in vitro*
330 (Fig. 3A), we interrogated whether addition of this cytokine in cultured wild type IEL modifies
331 their gene expression profile. For this purpose, we cultured FACS-enriched CD45$^+$ IEL from wild
332 type mice in the presence or absence of osteopontin. Twenty-four hours post-culture, cells were
333 collected, RNA extracted, sequenced and the gene expression profile determined. As recovery of
334 sufficient cells for gene expression profile analysis after 24 h of culture from individual IEL
335 populations was limiting, total CD45$^+$ IEL were used as an alternative approach. Gene set
336 enrichment analysis (GSEA) revealed that IEL cultured in the presence of recombinant osteopontin
337 express genes associated with retinoid X receptor (RXR) functions (Supplemental Fig. 2C and D).
338 GSEA also showed that IEL cultured in media alone present enriched pathways related to
339 apoptosis, degradation of p27/p21 and downregulation of genes in regulatory T cells
340 (Supplemental Fig. 2C and D). These results indicate that *in vitro* IEL exposure to osteopontin has
341 an impact on IEL gene transcription and modifies gene sets related to cell survival.

342

343 *Osteopontin does not influence T cell migration into the epithelium but maintains homeostasis of*
344 *TCRβ$^+$CD4$^+$ and TCRβ$^+$CD4$^+$CD8α$^+$ IEL*

345 Because some IEL populations are derived from conventional CD4$^+$ and CD8$^+$ T cells, we
346 investigated whether osteopontin is important for the relocation of these cells into the IEL
347 compartment. To test this hypothesis, we adoptively transferred total spleen T cells from WT mice
348 into Rag-2$^{-/-}$ or Spp-1$^{-/-}$Rag-2$^{-/-}$ recipient mice, and after 7 days we determined the number of cells
349 migrating into the intestinal epithelium. Fig. 4A (top) shows the gating strategy to identify cells
350 derived from donor mice. Both TCRβ$^+$CD4$^+$ and TCRβ$^+$CD8α$^+$ cells migrated similarly into the
351 epithelium of Rag-2$^{-/-}$ or Spp-1$^{-/-}$Rag-2$^{-/-}$ recipient mice (Fig. 4A, bottom), indicating that
352 osteopontin in the recipient mice does not influence the migration of these cells into the intestinal
353 mucosa. Interestingly, reconstitution analysis of Spp-1$^{-/-}$Rag-2$^{-/-}$ recipient mice at 28 days post
354 transfer showed a reduction in the total number of TCRβ$^+$CD4$^+$ and TCRβ$^+$CD4$^+$CD8α$^+$ cells but
355 not TCRβ$^+$CD8αβ$^+$ IEL (Fig. 4B), which resembled what was observed in naïve Spp-1-deficient
356 mice (Fig. 1B and Supplemental Fig. 1B). To prevent the development of intestinal inflammation
357 in Rag-2$^{-/-}$ recipient mice, we transferred total T cells, which includes regulatory T cells. To our
358 surprise, Spp-1$^{-/-}$Rag-2$^{-/-}$ recipient mice lost more weight than Rag-2$^{-/-}$ mice (Fig. 4C) and
359 presented increased colon inflammation (Fig. 4D). The impact of ostopontin produced by donor-
360 derived cells in IEL reconstitution and disease development was minimal, as determined by total
361 colon osteopontin mRNA expression prior to, and after 28 days post T cell transfer (Fig. 4E).

362 To interrogate why Spp-1$^{-/-}$Rag-2$^{-/-}$ mice developed intestinal inflammation when
363 regulatory T cells were present in the inoculum, we investigated the fate of regulatory T cells in
364 the presence or absence of osteopontin. Regulatory T cells are known to express CD44, which

365 when ligated, promotes sustained Foxp3 expression (49). Thus, we hypothesized that binding of
366 osteopontin to CD44 is a potential signal that maintains proper Foxp3 expression. To test this
367 possibility, we cultured total T cells from the intestines of RFP-Foxp3 mice in the presence or
368 absence of osteopontin, with or without anti-CD44. After 72 h of culture, there was an increase in
369 the percentage of RFP^+ cells in the presence of osteopontin, which was blunted with the addition
370 of anti-CD44 antibodies (Fig. 5A). Figure 5B shows the combined fold increase over untreated
371 cells.

372 To test whether osteopontin sustains Foxp3 expression *in vivo*, we sorted splenic RFP^+
373 cells from RFP-Foxp3 reporter mice and adoptively transferred them into Rag-$2^{-/-}$ or Spp-$1^{-/-}$Rag-
374 $2^{-/-}$ recipient mice. Eight weeks after transfer, IEL were isolated and the percentage of donor-
375 derived ($CD45^+TCR\beta^+CD4^+$) RFP^+ cells was determined (Fig. 5C). Rag-$2^{-/-}$ mice presented a trend
376 of higher percentage of donor-derived cells in the IEL compartment than Spp-$1^{-/-}$Rag-$2^{-/-}$ recipient
377 mice (Fig. 5D). Approximately 10% of the donor-derived cells from Rag-$2^{-/-}$ recipient mice
378 remained RFP^+, whereas only 4% of cells recovered from Spp-$1^{-/-}$Rag-$2^{-/-}$ recipient mice remained
379 RFP^+ (Fig. 5E). These results indicate that osteopontin sustains Foxp3 expression in regulatory T
380 cells in the IEL compartment, possible mediated by CD44 ligation, which significantly impacts
381 the development of intestinal inflammation.

382 To test whether CD44 expression, as one of the receptors for osteopontin on T cells, is
383 critical for prevention of experimental colitis, we adoptively transferred total T cells from $CD44^{-/-}$
384 donor mice into Rag-$2^{-/-}$ and Spp-$1^{-/-}$Rag-$2^{-/-}$ recipient mice. Rag-$2^{-/-}$ mice that received total spleen
385 T cells from WT mice did not lose weight, whereas Rag-$2^{-/-}$ and Spp-$1^{-/-}$Rag-$2^{-/-}$ recipient mice that
386 received spleen cells from $CD44^{-/-}$ donor mice lost weight comparably starting at 2 weeks post

387 transfer (Supplemental Fig. 3A), with clear signs of intestinal inflammation (Supplemental Fig.
388 3B).

389 Overall, these results show that osteopontin is not involved in the migration of adoptively
390 transferred conventional T cells into the intestinal epithelium, but sustains proper TCRβ^+CD4$^+$ and
391 TCRβ^+CD4$^+$CD8$^+$ cell numbers once in the IEL compartment. Moreover, the lack of osteopontin
392 in recipient mice results in development of colitis, even in the presence of regulatory T cells in the
393 inoculum. A similar outcome was observed when CD44-deficient T cells were transferred into
394 Rag-2$^{-/-}$ or Spp-1$^{-/-}$Rag-2$^{-/-}$ recipient mice, highlighting the importance of the osteopontin-CD44
395 interaction in intestinal homeostasis.

396

397 *iCD8α cell-derived osteopontin increases IEL survival*

398 iCD8α cells are a population of TCR^{neg} IEL involved in different immunological roles and are
399 known as an important source of osteopontin in the intestines (8). Recently, it has been shown that
400 survival of TCR^{neg} ILC1-like IEL depends in part on iCD8α cells, an effect most likely associated
401 with the production of osteopontin by these cells (36). To determine whether the survival of TCR$^+$
402 IEL populations is dependent on iCD8α cell-derived osteopontin, we performed experiments in
403 which the source of osteopontin is confined to a specific IEL population (iCD8α, TCRβ^+ or
404 TCR$\gamma\delta^+$ cells). Then, these individual IEL populations were co-cultured in the presence of total
405 IEL derived from osteopontin-deficient mice. After 4 h of culture, cells were stained for annexin
406 V and the increased in survival was calculated as indicated in the Materials and method section.
407 As shown in Fig. 6A, addition of osteopontin-competent iCD8α cells to the IEL culture resulted
408 in an increased survival (over IEL cultured in the absence of iCD8α cells) of almost 30% for
409 TCR$\gamma\delta^+$ and TCRβ^+CD8$\alpha\alpha^+$ IEL, whereas there was variable survival increase for unfractionated

410 TCRβ^+, and the IEL subpopulations TCRβ^+CD4$^+$, TCRβ^+CD4$^+$CD8α^+ and TCRβ^+CD8$\alpha\beta^+$.
411 Survival was reduced by addition of anti-osteopontin antibodies, indicating that iCD8α cell-
412 derived osteopontin was responsible for the observed increase in survival. A previous report
413 indicated that TCRβ^+ and TCR$\gamma\delta^+$ IEL also produce osteopontin (35). To determine whether these
414 IEL populations promote *in vitro* survival of IEL, we performed a similar experiment but the
415 potential source of osteopontin were TCRβ^+ or TCR$\gamma\delta^+$ IEL (Fig. 6B and C). TCRβ^+ IEL were
416 capable of stimulate survival of only TCR$\gamma\delta^+$ IEL and addition of anti-osteopontin antibodies
417 blunted the survival below the levels of cells cultured alone. For other IEL population, the addition
418 of TCRβ^+ IEL from osteopontin-competent mice did not enhance IEL survival (Fig. 6B). When
419 TCR$\gamma\delta^+$ IEL were used as the source of osteopontin, these cells were capable of increasing only
420 the survival of TCRβ^+CD8$\alpha\beta^+$ IEL. To determine that the osteopontin-competent cells have
421 similar viability after 4 h of culture, we analyzed their annexin V profile. As indicated in
422 Supplemental Fig. 4A, iCD8α, TCRβ^+ and TCR$\gamma\delta^+$ IEL presented low percentage of annexin V-
423 positive cells, and these percentages were similar among the 3 different type of IEL. To determine
424 the production of osteopontin from each cell type in these co-cultures, we recovered the
425 supernatants and measured osteopontin concentration by ELISA. As expected, osteopontin was
426 not detected in supernatants from CD45$^+$ IEL derived from Spp-1$^{-/-}$ mice cultured alone, but was
427 readily detectable in cultures containing iCD8α cells (Supplemental Fig. 4A). On the other hand,
428 osteopontin was not detected in the supernatants that included TCRβ^+ or TCR$\gamma\delta^+$ IEL from
429 osteopontin-competent mice (Supplemental Fig. 4A). These results suggest that the observed
430 increased survival promoted by TCRβ^+ and TCR$\gamma\delta^+$ IEL may not be completely dependent on
431 osteopontin, since this protein was not detected in the supernatants. Overall, these results indicate
432 that iCD8α cell-derived osteopontin is an important survival signal for IEL.

433 Intestinal epithelial cells are known to constitutively express low levels of osteopontin (25,
434 26), representing a potential source of this protein for the homeostasis of IEL. Because IEC rapidly
435 die in *in vitro* culture conditions, we determine their contribution to IEL homeostasis by analyzing
436 the IEL compartment of mice with conditional mutation of the osteopontin gene driven by the
437 villin promoter, which is preferentially expressed in IEC (Vill.Cre$^{+/-}$Spp-1$^{fl/fl}$). Expression of
438 osteopontin in IEC is ablated, but not in activated T cells, in Vill.Cre$^{+/-}$Spp-1$^{fl/fl}$ mice validating
439 the conditional mutation (Supplemental Fig. 4C). As shown in Fig. 7A and B, the absence of
440 osteopontin expression in IEC does not impact total small intestine or colon IEL cell numbers,
441 indicating that IEC-derived osteopontin does not contribute to the homeostasis of most IEL
442 populations.
443

444 **Discussion**

445 Intestinal IEL reside in the unique environment of the IEC monolayer. In this anatomical location,
446 IEL are poised as one the first immunological defenses against potential pathogens from the
447 intestinal lumen. In order to fulfill their immunological roles, IEL need to maintain their
448 homeostasis. However, because IEL represent a diverse population of lymphoid cells,
449 requirements for their homeostasis within the epithelium may depend on the particular type of IEL.
450 For example, TCR$\gamma\delta^+$ IEL require IL-7 for their proper development whereas other IEL are not
451 affected by this cytokine (50). On the other hand, IL-15 deficiency does not disturb TCR$\gamma\delta^+$ IEL
452 but has a significant impact on TCR$\alpha\beta^+$CD8$\alpha\alpha^+$, iCD8α and iCD3$^+$ IEL (7, 8, 51). The results
453 presented in this report indicate that osteopontin is important for the homeostasis of many different
454 IEL subpopulations. This implies that despite having different developmental pathways and
455 cytokine requirements, the presence of osteopontin in the epithelium ensures proper homeostasis
456 of most types of intestinal IEL.

457 Osteopontin-mediated T cell survival has been documented previously. For example,
458 concanavalin A-activated T cells from lymph nodes show reduced levels of cell death in the
459 presence of osteopontin (33). It is important to note that this report demonstrated a pivotal role for
460 osteopontin as an enhancer for the survival of effector Th17 cells, particularly during brain
461 inflammation (33). However, whereas this group studied differentiated Th17 cells in the context
462 of brain inflammation our results are based on IEL in naïve animals. In the present report, using
463 an *in vitro* system, we show that TCR$^+$ IEL rapidly die in the absence of osteopontin, whereas the
464 presence of this cytokine increased their *in vitro* survival (Fig. 3). Interestingly, each IEL
465 subpopulation presented different survival kinetics, but appeared to have a similar survival
466 requirement for osteopontin. Strikingly, the effect of osteopontin was only observed at 48 h

467 (TCRβ^+CD4$^+$ and TCRβCD4$^+$CD8α^+ IEL) or 72 h (TCR$\gamma\delta^+$ and TCRβ^+CD8α^+ IEL). The reason
468 why the osteopontin effect is only observed at later time points and not at 24 h is not clear.
469 However, it is possible that as IEL are exposed to exogenous osteopontin during the first hours of
470 culture, there is a decrease in their annexin V profile (as shown in Fig. 6), however their resilience
471 to cell death is delayed, which is observed at later time points.

472 CD44 is known to be one of the receptors for osteopontin, and the interaction between
473 these two molecules promotes adhesion and chemotaxis of bone marrow cells (52), increases
474 growth of cancer cell lines (53), stimulates survival of pro-B cell lines (54), induces production of
475 IL-10 in T cells (55), and protects T cell hybridomas from activated-induced cell death (56), among
476 other functions. Despite the many roles attributed to the osteopontin-CD44 interaction, its role in
477 IEL survival has not been investigated. IEL are considered to be in a "semi-activated" state (57),
478 and most of these cells express CD44. Therefore, it is reasonable to speculate that some IEL
479 subpopulations receive survival signals via the interaction between osteopontin and CD44.
480 Interestingly, splenic CD44$^+$ T cell survival was not increased by the addition of osteopontin *in*
481 *vitro*, which suggests that osteopontin may not affect all T cells expressing CD44. We also show
482 that the IEL survival promoted by osteopontin can be blunted by addition of anti-CD44 antibodies
483 (Fig. 3), underscoring the importance of the osteopontin-CD44 interaction in IEL biology.
484 However, it is noteworthy that IEL deficiencies in CD44$^{-/-}$ mice do not faithfully resemble those
485 observed in Spp-1$^{-/-}$ mice, suggesting that in the absence of CD44, other receptors may bind
486 osteopontin to stimulate survival of specific IEL subpopulations.

487 In the adoptive transfer experiments reported here, donor CD4 T cells from WT mice
488 reconstituted the IEL compartment of Spp-1$^{-/-}$Rag-2$^{-/-}$ recipient mice less efficiently than in Rag-
489 2$^{-/-}$ recipient mice, suggesting that an environment capable of producing osteopontin is important

490 for proper cell reconstitution in the intestines. However, transfer of T cells from osteopontin-
491 deficient donor mice into Rag-2$^{-/-}$ recipient mice resulted in reduced survival rates in the spleen
492 and lymph nodes in comparison to donor T cells from wild type donor mice (31). These results
493 indicate that intrinsic T cell-derived osteopontin is critical for normal cell reconstitution in
494 secondary lymphoid organs whereas T cells present in the IEL compartment depend on osteopontin
495 from the environment.

496 Adoptive transfer of total spleen T cells into immunodeficient hosts, such as Rag-2$^{-/-}$ mice,
497 normally results in cellular reconstitution and protection from T cell-mediated colitis due to the
498 presence of regulatory T cells (58, 59). Surprisingly, when recipient Rag-2$^{-/-}$ mice were deficient
499 in osteopontin (Rag-2$^{-/-}$Spp-1$^{-/-}$ animals), mice developed colitis even in the presence of regulatory
500 T cells (Fig. 4), raising the possibility that environmental osteopontin is important for maintaining
501 regulatory T cell function, as shown in Fig. 5.

502 If most IEL subpopulations require osteopontin for their homeostasis, what are the cellular
503 sources for this protein in the intestines? IEC produce osteopontin, and its expression increases
504 during inflammation (25, 26). Other sources of osteopontin are within the IEL compartment, which
505 appear to be confined to IEL expressing CD8α, including TCRγδ^{+}, TCRβ^{+}, and iCD8α cells (8,
506 35). We have previously shown that the survival of TCR^{neg} ILC1-like IEL (NKp46^{+}NK1.1^{+})
507 depends on iCD8α cell-derived osteopontin (36). Our previous publication and the results
508 presented herein provide significance evidence to suggest that one of the main roles for iCD8α
509 cells is the maintenance of proper IEL homeostasis. iCD8α cells constitute around 2 to 5% of the
510 total IEL compartment. Considering that IEL are interspaced between IEC at an approximate ratio
511 of 1 IEL for 10 IEC (2), how do iCD8α cells promote osteopontin-dependent survival of IEL in
512 the monolayer of intestinal epithelial cells? It is known that some IEL, like TCRγδ^{+} cells scan the

513 intestinal epithelium by moving out through the basal section of the epithelium and entering the
514 IEC monolayer in another location (60). Therefore, it is possible that iCD8α cells use a similar
515 mechanism to scan the monolayer, reach other IEL and provide needed osteopontin to other cells.
516 In the past few years, the role of osteopontin in the etiology of human diseases has been
517 greatly appreciated. For example, recent work has investigated the use of neutralizing anti-
518 osteopontin antibodies as a therapeutic with preclinical studies currently underway (ref. in (61)).
519 Studies such as the one described herein show that osteopontin neutralization may affect IEL
520 homeostasis in individuals with non-gastrointestinal tract disorders, but may be beneficial for IBD
521 patients. Osteopontin appears to be a critical molecule with multiple effects, one of them
522 supporting proper IEL homeostasis, and therefore additional studies are needed to better
523 understand its function and how it affects the biology of the mucosal immune system.
524

525 **Acknowledgments**

526 We thank the Flow Cytometry Shared Resource for technical help and guidance; the
527 Translational Pathology Shared Resource for tissue processing; the Vanderbilt Genome Editing
528 Resource, especially Dr. Leesa Sampson for her outstanding help for the generation of the Spp-
529 $1^{fl/fl}$ mice. We are thankful to Theresa Rogers, RN, for her help securing human blood and tissue
530 samples. We thank Dr. Luc Van Kaer for reviewing the manuscript
531

532 **References**

533 1. Cheroutre, H., F. Lambolez, and D. Mucida. 2011. The light and dark sides of intestinal
534 intraepithelial lymphocytes. *Nat Rev Immunol* 11: 445-456.
535 2. Olivares-Villagomez, D., and L. Van Kaer. 2017. Intestinal Intraepithelial Lymphocytes:
536 Sentinels of the Mucosal Barrier. *Trends Immunol*.
537 3. Van Kaer, L., and D. Olivares-Villagomez. 2018. Development, Homeostasis, and
538 Functions of Intestinal Intraepithelial Lymphocytes. *J Immunol* 200: 2235-2244.
539 4. Fuchs, A., W. Vermi, J. S. Lee, S. Lonardi, S. Gilfillan, R. D. Newberry, M. Cella, and
540 M. Colonna. 2013. Intraepithelial type 1 innate lymphoid cells are a unique subset of IL-
541 12- and IL-15-responsive IFN-gamma-producing cells. *Immunity* 38: 769-781.
542 5. Talayero, P., E. Mancebo, J. Calvo-Pulido, S. Rodriguez-Munoz, I. Bernardo, R. Laguna-
543 Goya, F. L. Cano-Romero, A. Garcia-Sesma, C. Loinaz, C. Jimenez, I. Justo, and E. Paz-
544 Artal. 2016. Innate Lymphoid Cells Groups 1 and 3 in the Epithelial Compartment of
545 Functional Human Intestinal Allografts. *Am J Transplant* 16: 72-82.
546 6. Van Acker, A., K. Gronke, A. Biswas, L. Martens, Y. Saeys, J. Filtjens, S. Taveirne, E.
547 Van Ammel, T. Kerre, P. Matthys, T. Taghon, B. Vandekerckhove, J. Plum, I. R. Dunay,
548 A. Diefenbach, and G. Leclercq. 2017. A Murine Intestinal Intraepithelial NKp46-
549 Negative Innate Lymphoid Cell Population Characterized by Group 1 Properties. *Cell*
550 *Rep* 19: 1431-1443.
551 7. Ettersperger, J., N. Montcuquet, G. Malamut, N. Guegan, S. Lopez-Lastra, S. Gayraud,
552 C. Reimann, E. Vidal, N. Cagnard, P. Villarese, I. Andre-Schmutz, R. Gomes
553 Domingues, C. Godinho-Silva, H. Veiga-Fernandes, L. Lhermitte, V. Asnafi, E.
554 Macintyre, C. Cellier, K. Beldjord, J. P. Di Santo, N. Cerf-Bensussan, and B. Meresse.

555 2016. Interleukin-15-Dependent T-Cell-like Innate Intraepithelial Lymphocytes Develop
556 in the Intestine and Transform into Lymphomas in Celiac Disease. *Immunity* 45: 610-625.
557 8. Van Kaer, L., H. M. Algood, K. Singh, V. V. Parekh, M. J. Greer, M. B. Piazuelo, J. H.
558 Weitkamp, P. Matta, R. Chaturvedi, K. T. Wilson, and D. Olivares-Villagomez. 2014.
559 CD8alphaalpha(+) Innate-Type Lymphocytes in the Intestinal Epithelium Mediate
560 Mucosal Immunity. *Immunity* 41: 451-464.
561 9. Edelblum, K. L., G. Singh, M. A. Odenwald, A. Lingaraju, K. El Bissati, R. McLeod, A.
562 I. Sperling, and J. R. Turner. 2015. gammadelta Intraepithelial Lymphocyte Migration
563 Limits Transepithelial Pathogen Invasion and Systemic Disease in Mice.
564 *Gastroenterology* 148: 1417-1426.
565 10. Ismail, A. S., K. M. Severson, S. Vaishnava, C. L. Behrendt, X. Yu, J. L. Benjamin, K.
566 A. Ruhn, B. Hou, A. L. DeFranco, F. Yarovinsky, and L. V. Hooper. 2011. Gammadelta
567 intraepithelial lymphocytes are essential mediators of host-microbial homeostasis at the
568 intestinal mucosal surface. *Proc Natl Acad Sci U S A* 108: 8743-8748.
569 11. Inagaki-Ohara, K., T. Chinen, G. Matsuzaki, A. Sasaki, Y. Sakamoto, K. Hiromatsu, F.
570 Nakamura-Uchiyama, Y. Nawa, and A. Yoshimura. 2004. Mucosal T cells bearing
571 TCRgammadelta play a protective role in intestinal inflammation. *J Immunol* 173: 1390-
572 1398.
573 12. Lepage, A. C., D. Buzoni-Gatel, D. T. Bout, and L. H. Kasper. 1998. Gut-derived
574 intraepithelial lymphocytes induce long term immunity against Toxoplasma gondii. *J*
575 *Immunol* 161: 4902-4908.
576 13. Masopust, D., D. Choo, V. Vezys, E. J. Wherry, J. Duraiswamy, R. Akondy, J. Wang, K.
577 A. Casey, D. L. Barber, K. S. Kawamura, K. A. Fraser, R. J. Webby, V. Brinkmann, E.

578 C. Butcher, K. A. Newell, and R. Ahmed. 2010. Dynamic T cell migration program
579 provides resident memory within intestinal epithelium. *J Exp Med* 207: 553-564.
580 14. Masopust, D., J. Jiang, H. Shen, and L. Lefrancois. 2001. Direct analysis of the dynamics
581 of the intestinal mucosa CD8 T cell response to systemic virus infection. *J Immunol* 166:
582 2348-2356.
583 15. Das, G., M. M. Augustine, J. Das, K. Bottomly, P. Ray, and A. Ray. 2003. An important
584 regulatory role for CD4+CD8 alpha alpha T cells in the intestinal epithelial layer in the
585 prevention of inflammatory bowel disease. *Proc Natl Acad Sci U S A* 100: 5324-5329.
586 PMC1535703.
587 16. Kumar, A. A., A. G. Delgado, M. B. Piazuelo, L. Van Kaer, and D. Olivares-Villagomez.
588 2017. Innate CD8alphaalpha(+) lymphocytes enhance anti-CD40 antibody-mediated
589 colitis in mice. *Immun Inflamm Dis* 5: 109-123.
590 17. Franzen, A., and D. Heinegard. 1985. Isolation and characterization of two sialoproteins
591 present only in bone calcified matrix. *Biochem J* 232: 715-724.
592 18. Prince, C. W., T. Oosawa, W. T. Butler, M. Tomana, A. S. Bhown, M. Bhown, and R. E.
593 Schrohenloher. 1987. Isolation, characterization, and biosynthesis of a phosphorylated
594 glycoprotein from rat bone. *J Biol Chem* 262: 2900-2907.
595 19. Di Bartolomeo, M., F. Pietrantonio, A. Pellegrinelli, A. Martinetti, L. Mariani, M. G.
596 Daidone, E. Bajetta, G. Pelosi, F. de Braud, I. Floriani, and R. Miceli. 2016. Osteopontin,
597 E-cadherin, and beta-catenin expression as prognostic biomarkers in patients with
598 radically resected gastric cancer. *Gastric Cancer* 19: 412-420.

599 20. Giachelli, C. M., N. Bae, M. Almeida, D. T. Denhardt, C. E. Alpers, and S. M. Schwartz.
600 1993. Osteopontin is elevated during neointima formation in rat arteries and is a novel
601 component of human atherosclerotic plaques. *J Clin Invest* 92: 1686-1696.
602 21. Icer, M. A., and M. Gezmen-Karadag. 2018. The multiple functions and mechanisms of
603 osteopontin. *Clin Biochem* 59: 17-24.
604 22. Oz, H. S., J. Zhong, and W. J. de Villiers. 2012. Osteopontin ablation attenuates
605 progression of colitis in TNBS model. *Dig Dis Sci* 57: 1554-1561.
606 23. Zhong, J., E. R. Eckhardt, H. S. Oz, D. Bruemmer, and W. J. de Villiers. 2006.
607 Osteopontin deficiency protects mice from Dextran sodium sulfate-induced colitis.
608 *Inflamm Bowel Dis* 12: 790-796.
609 24. Mishima, R., F. Takeshima, T. Sawai, K. Ohba, K. Ohnita, H. Isomoto, K. Omagari, Y.
610 Mizuta, Y. Ozono, and S. Kohno. 2007. High plasma osteopontin levels in patients with
611 inflammatory bowel disease. *J Clin Gastroenterol* 41: 167-172.
612 25. Sato, T., T. Nakai, N. Tamura, S. Okamoto, K. Matsuoka, A. Sakuraba, T. Fukushima, T.
613 Uede, and T. Hibi. 2005. Osteopontin/Eta-1 upregulated in Crohn's disease regulates the
614 Th1 immune response. *Gut* 54: 1254-1262.
615 26. Gassler, N., F. Autschbach, S. Gauer, J. Bohn, B. Sido, H. F. Otto, H. Geiger, and N.
616 Obermuller. 2002. Expression of osteopontin (Eta-1) in Crohn disease of the terminal
617 ileum. *Scand J Gastroenterol* 37: 1286-1295.
618 27. Masuda, H., Y. Takahashi, S. Asai, and T. Takayama. 2003. Distinct gene expression of
619 osteopontin in patients with ulcerative colitis. *J Surg Res* 111: 85-90.
620 28. Neuman, M. G. 2012. Osteopontin biomarker in inflammatory bowel disease, animal
621 models and target for drug discovery. *Dig Dis Sci* 57: 1430-1431.

622 29. Boumans, M. J., J. G. Houbiers, P. Verschueren, H. Ishikura, R. Westhovens, E.
623 Brouwer, B. Rojkovich, S. Kelly, M. den Adel, J. Isaacs, H. Jacobs, J. Gomez-Reino, G.
624 M. Holtkamp, A. Hastings, D. M. Gerlag, and P. P. Tak. 2012. Safety, tolerability,
625 pharmacokinetics, pharmacodynamics and efficacy of the monoclonal antibody
626 ASK8007 blocking osteopontin in patients with rheumatoid arthritis: a randomised,
627 placebo controlled, proof-of-concept study. *Annals of the rheumatic diseases* 71: 180-
628 185.
629 30. Lund, S. A., C. L. Wilson, E. W. Raines, J. Tang, C. M. Giachelli, and M. Scatena. 2013.
630 Osteopontin mediates macrophage chemotaxis via alpha4 and alpha9 integrins and
631 survival via the alpha4 integrin. *J Cell Biochem* 114: 1194-1202.
632 31. Leavenworth, J. W., B. Verbinnen, Q. Wang, E. Shen, and H. Cantor. 2015. Intracellular
633 osteopontin regulates homeostasis and function of natural killer cells. *Proc Natl Acad Sci*
634 *U S A* 112: 494-499.
635 32. Shinohara, M. L., H. J. Kim, J. H. Kim, V. A. Garcia, and H. Cantor. 2008. Alternative
636 translation of osteopontin generates intracellular and secreted isoforms that mediate
637 distinct biological activities in dendritic cells. *Proc Natl Acad Sci U S A* 105: 7235-7239.
638 33. Hur, E. M., S. Youssef, M. E. Haws, S. Y. Zhang, R. A. Sobel, and L. Steinman. 2007.
639 Osteopontin-induced relapse and progression of autoimmune brain disease through
640 enhanced survival of activated T cells. *Nat Immunol* 8: 74-83.
641 34. Ashkar, S., G. F. Weber, V. Panoutsakopoulou, M. E. Sanchirico, M. Jansson, S.
642 Zawaideh, S. R. Rittling, D. T. Denhardt, M. J. Glimcher, and H. Cantor. 2000. Eta-1
643 (osteopontin): an early component of type-1 (cell-mediated) immunity. *Science* 287: 860-
644 864.

645 35. Ito, K., A. Nakajima, Y. Fukushima, K. Suzuki, K. Sakamoto, Y. Hamazaki, K.
646 Ogasawara, N. Minato, and M. Hattori. 2017. The potential role of Osteopontin in the
647 maintenance of commensal bacteria homeostasis in the intestine. *PLoS One* 12:
648 e0173629.
649 36. Nazmi, A., K. L. Hoek, M. J. Greer, M. B. Piazuelo, N. Minato, and D. Olivares-
650 Villagomez. 2019. Innate CD8alphaalpha+ cells promote ILC1-like intraepithelial
651 lymphocyte homeostasis and intestinal inflammation. *PLoS One* 14: e0215883.
652 37. Quadros, R. M., H. Miura, D. W. Harms, H. Akatsuka, T. Sato, T. Aida, R. Redder, G. P.
653 Richardson, Y. Inagaki, D. Sakai, S. M. Buckley, P. Seshacharyulu, S. K. Batra, M. A.
654 Behlke, S. A. Zeiner, A. M. Jacobi, Y. Izu, W. B. Thoreson, L. D. Urness, S. L. Mansour,
655 M. Ohtsuka, and C. B. Gurumurthy. 2017. Easi-CRISPR: a robust method for one-step
656 generation of mice carrying conditional and insertion alleles using long ssDNA donors
657 and CRISPR ribonucleoproteins. *Genome biology* 18: 92.
658 38. Olivares-Villagomez, D., Y. V. Mendez-Fernandez, V. V. Parekh, S. Lalani, T. L.
659 Vincent, H. Cheroutre, and L. Van Kaer. 2008. Thymus leukemia antigen controls
660 intraepithelial lymphocyte function and inflammatory bowel disease. *Proc Natl Acad Sci*
661 *U S A* 105: 17931-17936. PMC2584730.
662 39. Hoek, K. L., P. Samir, L. M. Howard, X. Niu, N. Prasad, A. Galassie, Q. Liu, T. M.
663 Allos, K. A. Floyd, Y. Guo, Y. Shyr, S. E. Levy, S. Joyce, K. M. Edwards, and A. J.
664 Link. 2015. A cell-based systems biology assessment of human blood to monitor immune
665 responses after influenza vaccination. *PLoS One* 10: e0118528.
666 40. Weitkamp, J. H., T. Koyama, M. T. Rock, H. Correa, J. A. Goettel, P. Matta, K. Oswald-
667 Richter, M. J. Rosen, B. G. Engelhardt, D. J. Moore, and D. B. Polk. 2013. Necrotising

668 enterocolitis is characterised by disrupted immune regulation and diminished mucosal
669 regulatory (FOXP3)/effector (CD4, CD8) T cell ratios. *Gut* 62: 73-82.
670 41. Aranda, R., B. C. Sydora, P. L. McAllister, S. W. Binder, H. Y. Yang, S. R. Targan, and
671 M. Kronenberg. 1997. Analysis of intestinal lymphocytes in mouse colitis mediated by
672 transfer of CD4+, CD45RBhigh T cells to SCID recipients. *J Immunol* 158: 3464-3473.
673 42. Patro, R., G. Duggal, M. I. Love, R. A. Irizarry, and C. Kingsford. 2017. Salmon
674 provides fast and bias-aware quantification of transcript expression. *Nature methods* 14:
675 417-419.
676 43. Robinson, M. D., D. J. McCarthy, and G. K. Smyth. 2010. edgeR: a Bioconductor
677 package for differential expression analysis of digital gene expression data.
678 *Bioinformatics* 26: 139-140.
679 44. Subramanian, A., P. Tamayo, V. K. Mootha, S. Mukherjee, B. L. Ebert, M. A. Gillette,
680 A. Paulovich, S. L. Pomeroy, T. R. Golub, E. S. Lander, and J. P. Mesirov. 2005. Gene
681 set enrichment analysis: a knowledge-based approach for interpreting genome-wide
682 expression profiles. *Proc Natl Acad Sci U S A* 102: 15545-15550.
683 45. Yokosaki, Y., K. Tanaka, F. Higashikawa, K. Yamashita, and A. Eboshida. 2005.
684 Distinct structural requirements for binding of the integrins alphavbeta6, alphavbeta3,
685 alphavbeta5, alpha5beta1 and alpha9beta1 to osteopontin. *Matrix biology : journal of the*
686 *International Society for Matrix Biology* 24: 418-427.
687 46. Katagiri, Y. U., J. Sleeman, H. Fujii, P. Herrlich, H. Hotta, K. Tanaka, S. Chikuma, H.
688 Yagita, K. Okumura, M. Murakami, I. Saiki, A. F. Chambers, and T. Uede. 1999. CD44
689 variants but not CD44s cooperate with beta1-containing integrins to permit cells to bind

690 to osteopontin independently of arginine-glycine-aspartic acid, thereby stimulating cell
691 motility and chemotaxis. *Cancer Res* 59: 219-226.
692 47. Beura, L. K., S. E. Hamilton, K. Bi, J. M. Schenkel, O. A. Odumade, K. A. Casey, E. A.
693 Thompson, K. A. Fraser, P. C. Rosato, A. Filali-Mouhim, R. P. Sekaly, M. K. Jenkins, V.
694 Vezys, W. N. Haining, S. C. Jameson, and D. Masopust. 2016. Normalizing the
695 environment recapitulates adult human immune traits in laboratory mice. *Nature* 532:
696 512-516.
697 48. Smolewski, P., and T. Robak. 2011. Inhibitors of apoptosis proteins (IAPs) as potential
698 molecular targets for therapy of hematological malignancies. *Curr Mol Med* 11: 633-649.
699 49. Bollyky, P. L., B. A. Falk, S. A. Long, A. Preisinger, K. R. Braun, R. P. Wu, S. P.
700 Evanko, J. H. Buckner, T. N. Wight, and G. T. Nepom. 2009. CD44 costimulation
701 promotes FoxP3+ regulatory T cell persistence and function via production of IL-2, IL-
702 10, and TGF-beta. *J Immunol* 183: 2232-2241.
703 50. Maki, K., S. Sunaga, Y. Komagata, Y. Kodaira, A. Mabuchi, H. Karasuyama, K.
704 Yokomuro, J. I. Miyazaki, and K. Ikuta. 1996. Interleukin 7 receptor-deficient mice lack
705 gammadelta T cells. *Proc Natl Acad Sci U S A* 93: 7172-7177. PMC38955.
706 51. Kennedy, M. K., M. Glaccum, S. N. Brown, E. A. Butz, J. L. Viney, M. Embers, N.
707 Matsuki, K. Charrier, L. Sedger, C. R. Willis, K. Brasel, P. J. Morrissey, K. Stocking, J.
708 C. Schuh, S. Joyce, and J. J. Peschon. 2000. Reversible defects in natural killer and
709 memory CD8 T cell lineages in interleukin 15-deficient mice. *J Exp Med* 191: 771-780.
710 52. Weber, G. F., S. Ashkar, M. J. Glimcher, and H. Cantor. 1996. Receptor-ligand
711 interaction between CD44 and osteopontin (Eta-1). *Science* 271: 509-512.

712 53. Sun, S. J., C. C. Wu, G. T. Sheu, H. Y. Chang, M. Y. Chen, Y. Y. Lin, C. Y. Chuang, S.
713 L. Hsu, and J. T. Chang. 2016. Integrin beta3 and CD44 levels determine the effects of
714 the OPN-a splicing variant on lung cancer cell growth. *Oncotarget* 7: 55572-55584.
715 54. Lin, Y. H., and H. F. Yang-Yen. 2001. The osteopontin-CD44 survival signal involves
716 activation of the phosphatidylinositol 3-kinase/Akt signaling pathway. *J Biol Chem* 276:
717 46024-46030.
718 55. Murugaiyan, G., A. Mittal, and H. L. Weiner. 2008. Increased osteopontin expression in
719 dendritic cells amplifies IL-17 production by CD4+ T cells in experimental autoimmune
720 encephalomyelitis and in multiple sclerosis. *J Immunol* 181: 7480-7488.
721 56. Larkin, J., G. J. Renukaradhya, V. Sriram, W. Du, J. Gervay-Hague, and R. R.
722 Brutkiewicz. 2006. CD44 differentially activates mouse NK T cells and conventional T
723 cells. *J Immunol* 177: 268-279.
724 57. Montufar-Solis, D., T. Garza, and J. R. Klein. 2007. T-cell activation in the intestinal
725 mucosa. *Immunol Rev* 215: 189-201. PMC2754816.
726 58. Powrie, F., R. Correa-Oliveira, S. Mauze, and R. L. Coffman. 1994. Regulatory
727 interactions between CD45RBhigh and CD45RBlow CD4+ T cells are important for the
728 balance between protective and pathogenic cell-mediated immunity. *J Exp Med* 179: 589-
729 600. PMC2191378.
730 59. Powrie, F., M. W. Leach, S. Mauze, S. Menon, L. B. Caddle, and R. L. Coffman. 1994.
731 Inhibition of Th1 responses prevents inflammatory bowel disease in scid mice
732 reconstituted with CD45RBhi CD4+ T cells. *Immunity* 1: 553-562.

733 60. Hoytema van Konijnenburg, D. P., B. S. Reis, V. A. Pedicord, J. Farache, G. D. Victora,
734 and D. Mucida. 2017. Intestinal Epithelial and Intraepithelial T Cell Crosstalk Mediates a
735 Dynamic Response to Infection. *Cell* 171: 783-794 e713.
736 61. Farrokhi, V., J. R. Chabot, H. Neubert, and Z. Yang. 2018. Assessing the Feasibility of
737 Neutralizing Osteopontin with Various Therapeutic Antibody Modalities. *Sci Rep* 8:
738 7781.
739

740 **Figure legends**

741 Figure 1. Osteopontin-deficient mice have a reduced IEL compartment. (A) Gating strategy
742 utilized in this report. After gating on live cells, IEL were gated as indicated. (B) Total IEL
743 numbers from the small intestine (top) and colon (bottom) of WT and Spp-1$^{-/-}$ mice. Each dot
744 represents an individual mouse (n = 13). (C) Total cell numbers of the indicated populations in the
745 spleens from WT and Spp-1$^{-/-}$ mice (n = 8). Bars indicate SEM. (D) Total cell numbers of the
746 indicated populations in the lamina propria from WT and Spp-1$^{-/-}$ mice. Each dot represents an
747 individual mouse (n = 5). Data from (B) to (D) are representative of two to three independent
748 experiments. * $P<0.05$; ** $P<0.01$; **** $P<0.0001$ (Mann-Whitney U test).

749

750 Figure 2. Differential apoptosis and cell division in IEL from osteopontin-deficient mice. (A)
751 Annexin V staining of different small intestine IEL populations derived from WT and Spp-1$^{-/-}$
752 mice. After gating cells by size based on forward and side scatter profiles, cells were gated for the
753 expression of CD45 and other surface markers as indicated in Fig. 1A, and then analyzed for
754 annexin V and 7AAD staining. Dot plots show a representative sample. Summary is indicated in
755 the graphs. Data are representative of three independent experiments. Each dot represents an
756 individual sample (n = 8 to 10). (B) Ki67 intracellular staining of different small intestine IEL
757 populations derived from WT and Spp-1$^{-/-}$ mice. Cells were gated as in Figure 1A. Data are
758 representative from two independent experiments. Each dot represents an individual sample (n =
759 9 to 10). * $P<0.05$; ** $P<0.01$ (Mann-Whitney U test).

760

761 Figure 3. Osteopontin promotes *in vitro* IEL survival. (A) Indicated FACS-enriched IEL
762 populations from WT mice were left untreated or treated with recombinant murine osteopontin

763 (rOPN; 2 μg/ml), with or without anti-mouse CD44 (5 μg/ml). After the indicated time points, cell
764 survival was determined. Data are representative of three independent experiments. Biological
765 replicas consisted of two to three pooled IEL preparations from individual mice; each experiment
766 consisted of 3 biological replicas. (B) Enriched $CD45^+$ splenocytes were treated as in (A). Data
767 are representative of two independent experiments (n = 3). (C) FACS-enriched $TCR\beta^+CD44^+$
768 spleen cells from WT and Spp-$1^{-/-}$ mice were treated as in (A). Data are representative of two
769 independent experiments (n = 3). (D) Neonatal human IEL were incubated in the presence or
770 absence of recombinant human osteopontin (2 μg/ml) and anti-human CD44 (5μg/ml). After the
771 indicated time points, cell survival was determined. Each symbol represents an individual human:
772 circle, small intestine from 1-day old patient presenting volvulus and necrosis; square, ileum and
773 colon from 17-day old patient presenting necrotizing enterocolitis; triangle, jejunum from 12-day
774 old patient presenting necrotizing enterocolitis; diamond and hexagon, de-identified individuals.
775 (E) PBMC from adult humans were treated as in (D). Data are representative of two independent
776 experiments (n = 3). *P<0.05, **P<0.01, ***P<0.001 (One-way ANOVA).
777
778 Figure 4. Environmental osteopontin influences IEL reconstitution and colon inflammation.
779 Enriched total spleen T cells from WT mice were adoptively transferred into Rag-$2^{-/-}$ and Spp-$1^{-/-}$
780 Rag-$2^{-/-}$ mice. (A) Gating strategy to identify cells derived from donor mice (top). Representative
781 analysis of mice analyzed seven days after transfer (bottom). Dot plots show a representative
782 sample. Results are summarized in the graphs. $TCR\beta^+CD4^+CD8\alpha^+$ cells were not detected above
783 background at this time point in either group. Data are representative from two independent
784 experiments. Each dot represents an individual sample (n = 4 to 5). (B) The same analysis as in
785 (A) performed at 28 days post transfer. Dot plots show a representative sample. Results are

786 summarized in the graphs. Data are representative from three independent experiments. Each dot
787 represents an individual animal (n = 9). (C) Total weight change at 28 days post transfer of mice
788 treated as in (B). (D) Representative H&E stained samples of colon sections from the indicated
789 mice at 28 days (100X magnification). Graph indicates total histological score [immune cell
790 infiltration (3 points), loss of goblet cells (3 points), crypt damage (3 points) and epithelial
791 hyperplasia (3 points)]. For (C) and (D) data are representative from three independent
792 experiments, each dot represents an individual mouse (n = 9). (E) Total mRNA expression from
793 colons of naïve and T cell treated (28 days post-transfer) Rag-2$^{-/-}$ and Spp-1$^{-/-}$Rag-2$^{-/-}$ mice (n=3-
794 5). **P<0.01 (Mann-Whitney T test).
795
796 Figure 5. Osteopontin sustains Foxp3 expression. (A) Intestinal T cells from RFP-Foxp3 reporter
797 mice were isolated and cultured in the presence or absence of recombinant osteopontin (2 μg/ml)
798 and anti-CD44 (5 μg/ml). Seventy-two hours later, the percentage of RFP^{+} cells was determined
799 by flow cytometry. After excluding dead cells, dot plots were gated as CD45^{+}TCRβ^{+} cells. (B) Bar
800 graph indicates the fold change in CD4^{+}RFP^{+} cells in relation to the null group. Data are
801 representative of three independent experiments. (C) Enriched splenic RFP^{+} cells from RFP-Foxp3
802 reporter mice were adoptively transferred into Rag-2$^{-/-}$ and Spp-1$^{-/-}$Rag-2$^{-/-}$ recipient mice. Eight
803 weeks after transfer, IEL from small intestine were isolated and the percentage of RFP^{+}
804 determined. After excluding dead cells, plots were gated as indicated by the arrows. (D) Summary
805 of the percentage of donor-derived cells recovered; each dot represents an individual mouse. Data
806 are representative from three independent experiments. (E) Summary of the percentage of RFP^{+}
807 cells within the donor-derived cells. *P<0.05 (Mann-Whitney T test). rOPN = recombinant
808 osteopontin; aCD44 = anti-CD44 antibodies.

809

810 Figure 6. iCD8α cell-derived osteopontin promotes IEL survival. Enriched $CD45^+$ IEL from small
811 intestine and colon derived from Spp-$1^{-/-}$ mice were incubated in the presence or absence of
812 enriched iCD8α IEL (A), $TCR\beta^+$ IEL (B), or $TCR\gamma\delta^+$ IEL (C) from osteopontin-competent donors.
813 Some cells were cultured in the presence of anti-osteopontin antibodies (2 μg/ml). Four hours after
814 incubation, cells were stained for surface markers, including annexin V, and 7AAD. Cells were
815 gated as in Figure 2A. Graphs indicate "increased survival", which was determined as 100 - [% of
816 annexin V^+ read-out cells in co-culture x 100 / % of annexin V^+ cells cultured alone].

817

818 Figure 7. IEC-derived osteopontin does not promote IEL homeostasis. Small intestine (A) and
819 colon (B) IEL were isolated from Villin-$Cre^{-/-}$Spp-$1^{fl/fl}$ and Villin-$Cre^{+/-}$Spp-$1^{fl/fl}$ mice, and the
820 cellularity determined as indicated in Fig. 1A and B.

821

Figure 1

A

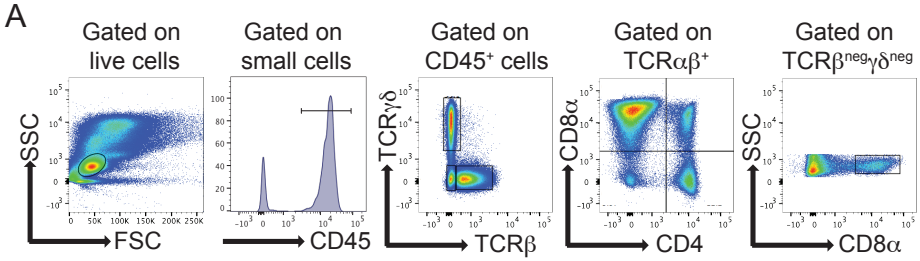

B

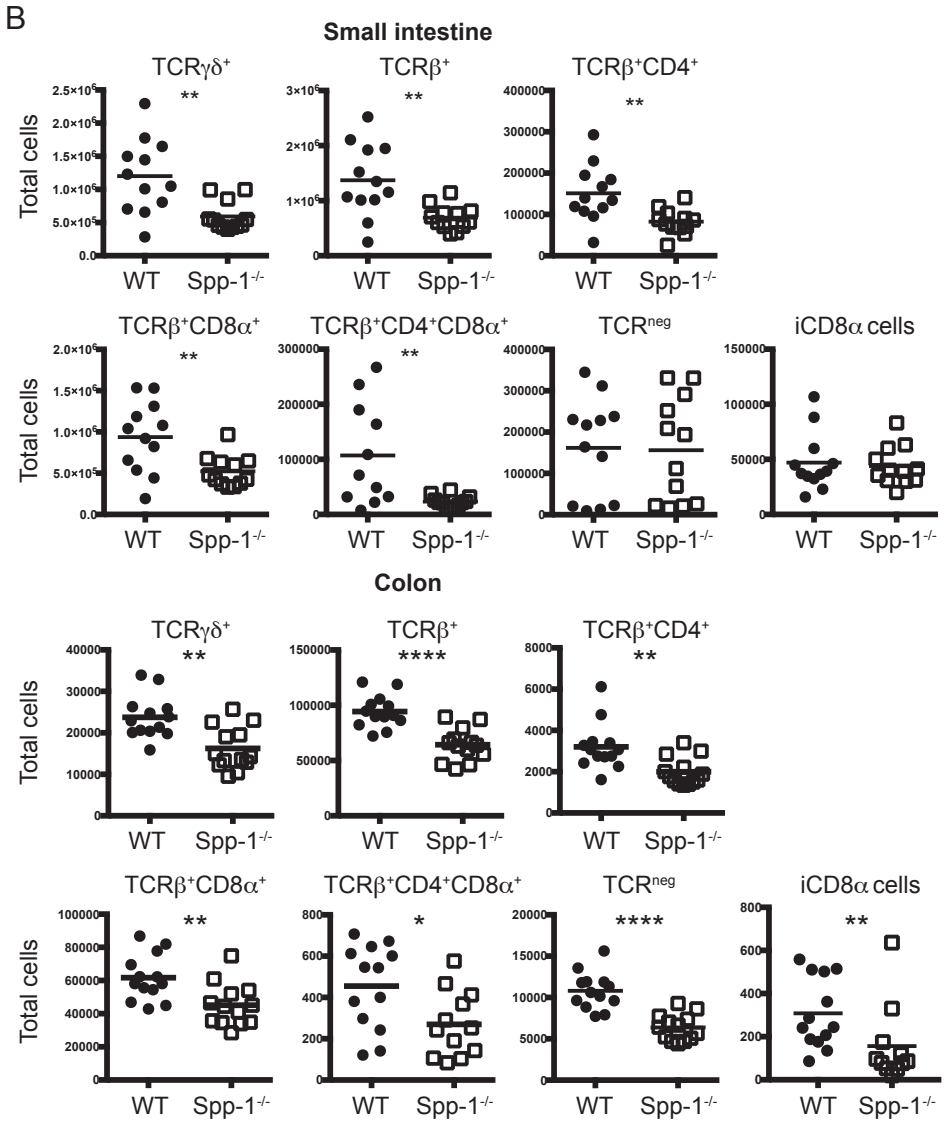

C

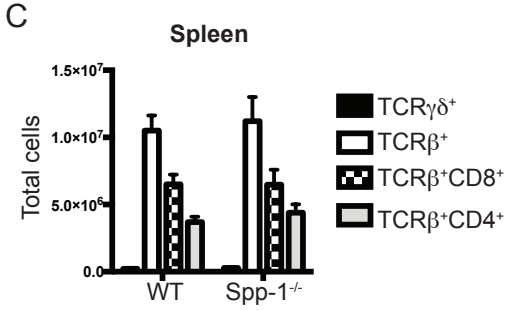

D

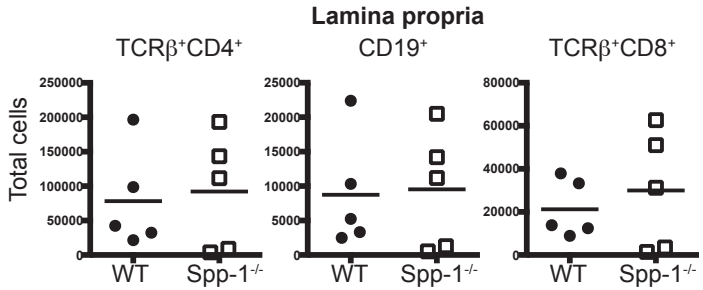

A

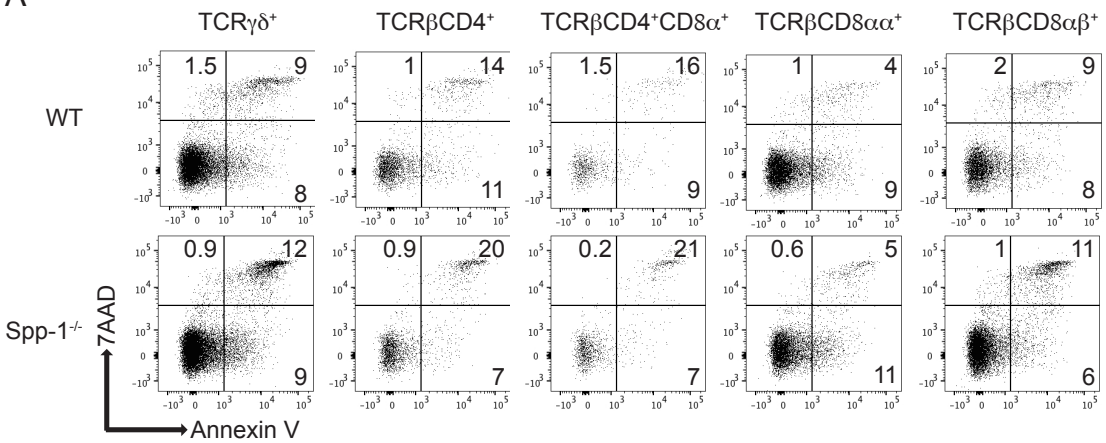
TCRγδ+
TCRβCD4+
TCRβCD4+CD8α+
TCRβCD8αα+
TCRβCD8αβ+
WT
Spp-1-/-
7AAD
Annexin V
1.5
9
8
1
14
11
1.5
16
9
1
4
9
2
9
8
0.9
12
9
0.9
20
7
0.2
21
7
0.6
5
11
1
11
6

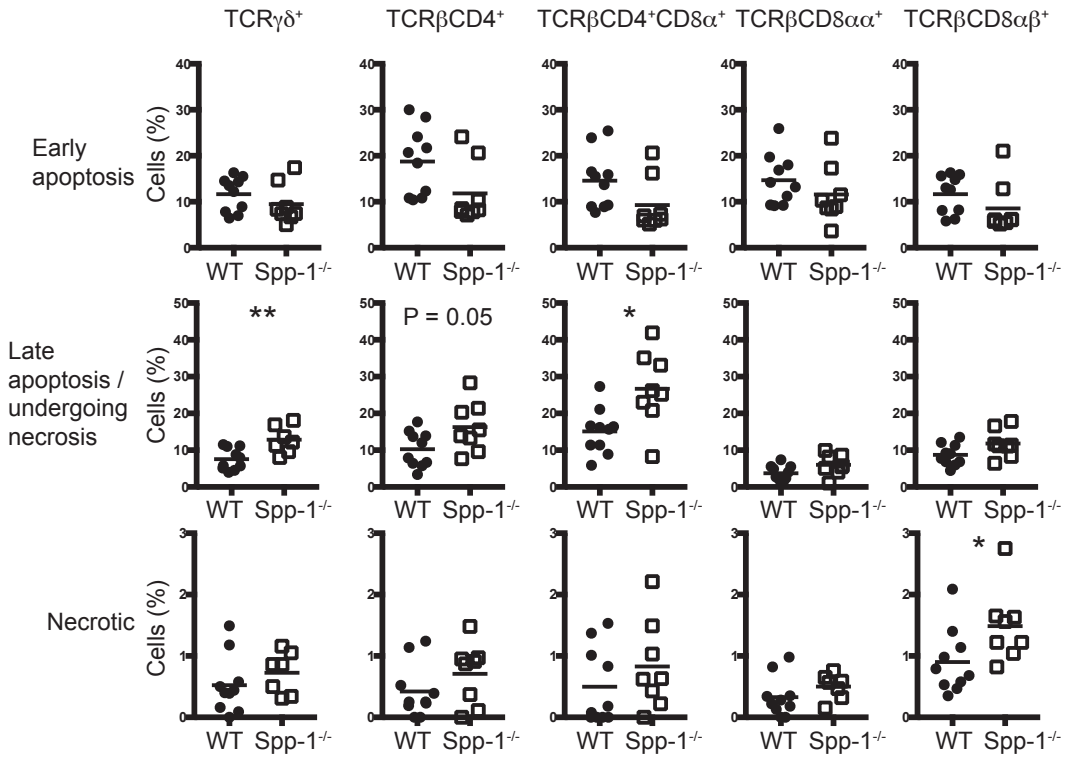
TCRγδ+
TCRβCD4+
TCRβCD4+CD8α+
TCRβCD8αα+
TCRβCD8αβ+
Early apoptosis
Late apoptosis / undergoing necrosis
Necrotic
Cells (%)
WT
Spp-1-/-
**
P = 0.05
*
*

B

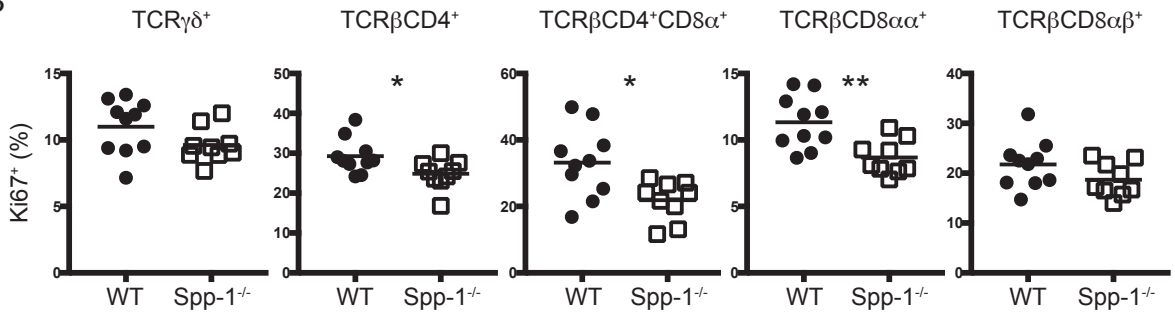
TCRγδ+
TCRβCD4+
TCRβCD4+CD8α+
TCRβCD8αα+
TCRβCD8αβ+
Ki67+ (%)
WT
Spp-1-/-
*
*
**

Figure 2

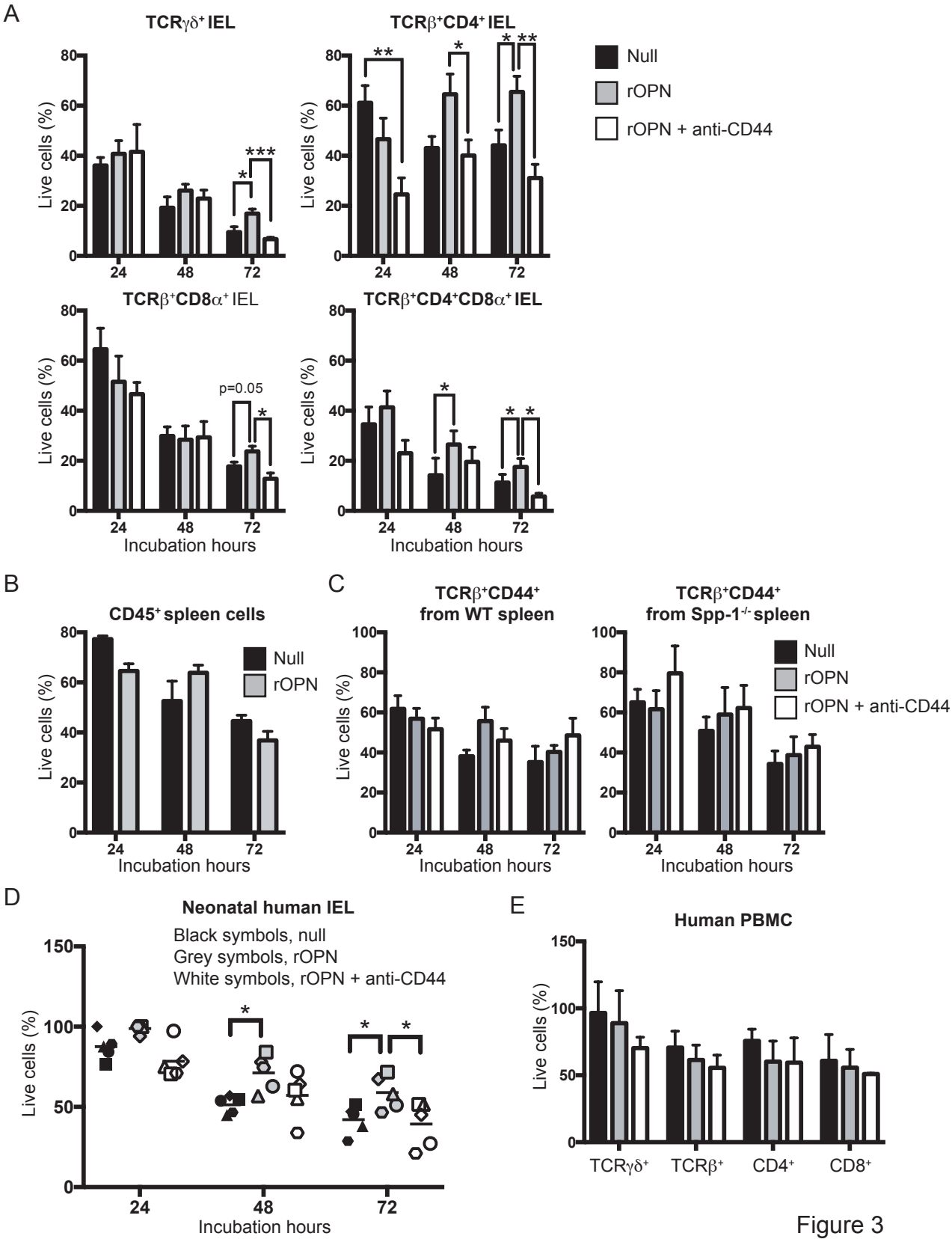
A
TCRγδ+ IEL
TCRβ+CD4+ IEL
TCRβ+CD8α+ IEL
TCRβ+CD4+CD8α+ IEL
Live cells (%)
Incubation hours
Null
rOPN
rOPN + anti-CD44
p=0.05
B
CD45+ spleen cells
C
TCRβ+CD44+ from WT spleen
TCRβ+CD44+ from Spp-1-/- spleen
D
Neonatal human IEL
Black symbols, null
Grey symbols, rOPN
White symbols, rOPN + anti-CD44
E
Human PBMC
TCRγδ+
TCRβ+
CD4+
CD8+

Figure 3

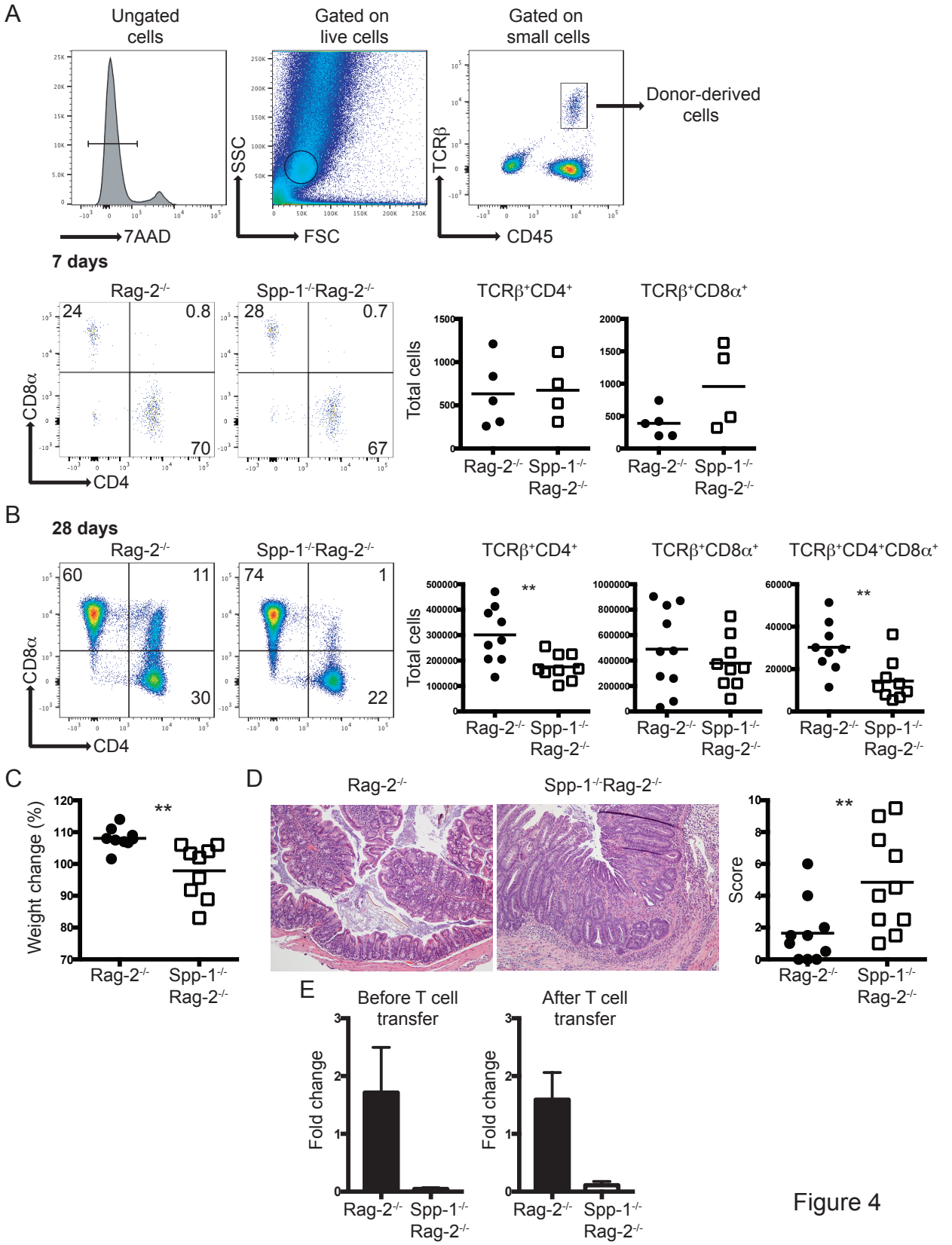
A
Ungated cells
Gated on live cells
Gated on small cells
Donor-derived cells
7AAD
SSC
FSC
TCRβ
CD45
7 days
Rag-2-/-
Spp-1-/-Rag-2-/-
24
0.8
70
28
0.7
67
CD8α
CD4
TCRβ+CD4+
TCRβ+CD8α+
Total cells
Rag-2-/-
Spp-1-/- Rag-2-/-
B
28 days
60
11
30
74
1
22
TCRβ+CD4+CD8α+
**
C
Weight change (%)
D
Score
E
Before T cell transfer
After T cell transfer
Fold change

Figure 4

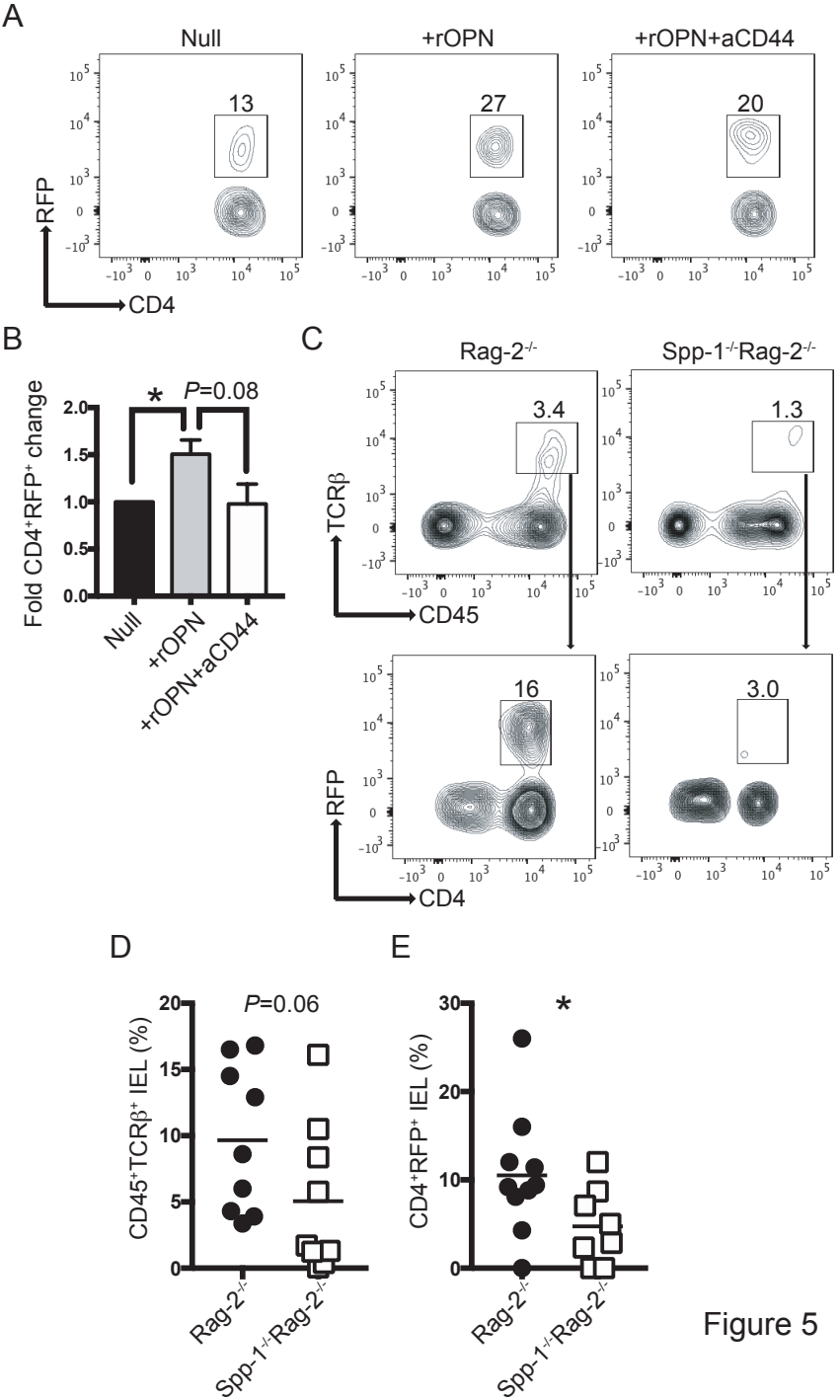
A
Null
+rOPN
+rOPN+aCD44
13
27
20
RFP
CD4
B
Fold CD4+RFP+ change
*
P=0.08
Null
+rOPN
+rOPN+aCD44
C
Rag-2-/-
Spp-1-/-Rag-2-/-
3.4
1.3
TCRβ
CD45
16
3.0
RFP
CD4
D
P=0.06
CD45+TCRβ+ IEL (%)
Rag-2-/-
Spp-1-/-Rag-2-/-
E
*
CD4+RFP+ IEL (%)
Rag-2-/-
Spp-1-/-Rag-2-/-

Figure 5

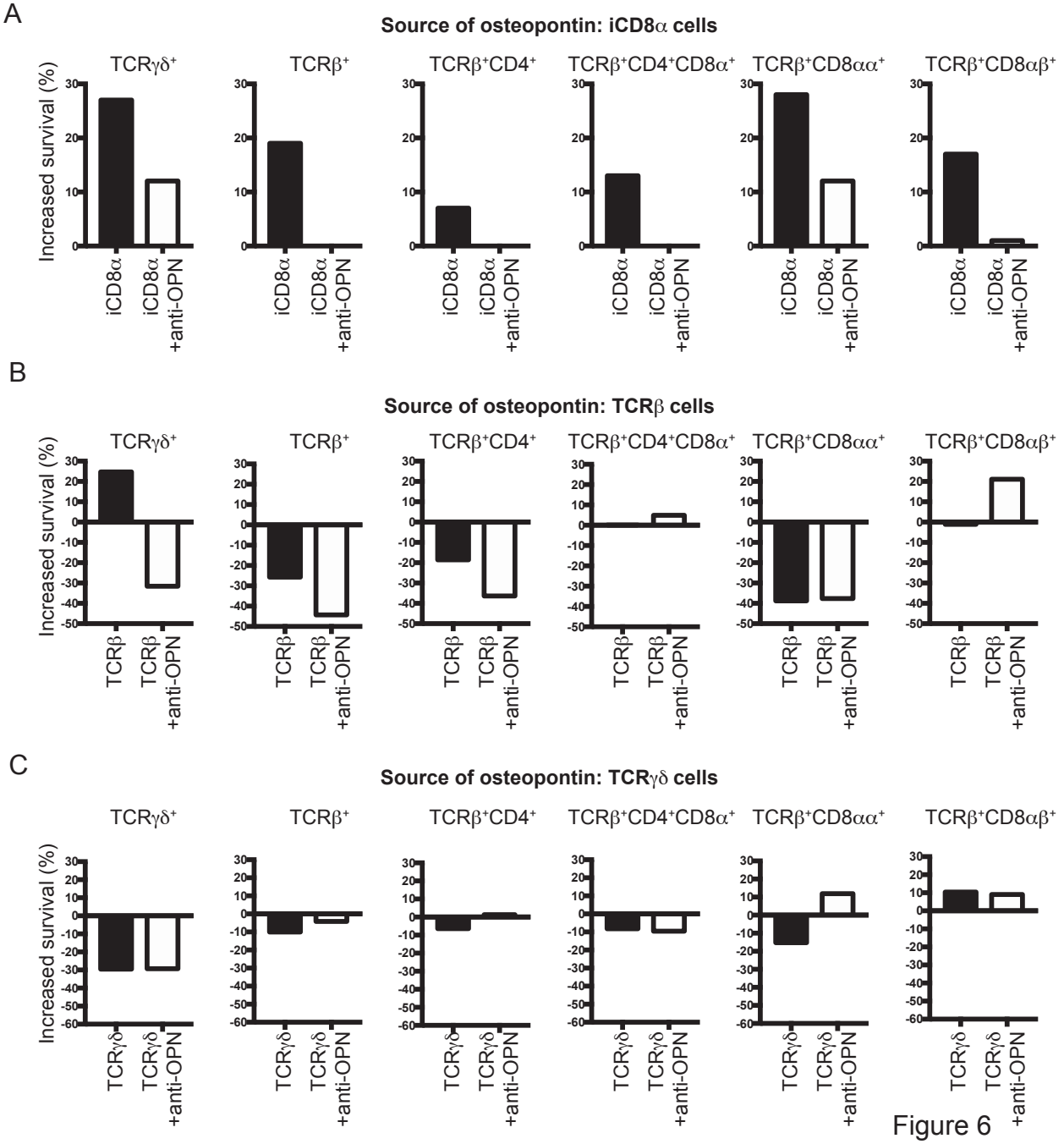
A
Source of osteopontin: iCD8α cells
Increased survival (%)
TCRγδ+
TCRβ+
TCRβ+CD4+
TCRβ+CD4+CD8α+
TCRβ+CD8αα+
TCRβ+CD8αβ+
iCD8α
iCD8α +anti-OPN
B
Source of osteopontin: TCRβ cells
TCRβ
TCRβ +anti-OPN
C
Source of osteopontin: TCRγδ cells
TCRγδ
TCRγδ +anti-OPN

Figure 6

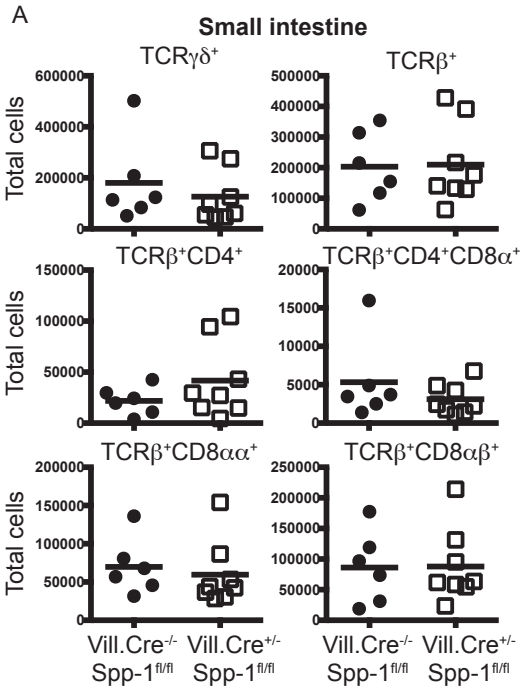
A
Small intestine
TCRγδ+
TCRβ+
TCRβ+CD4+
TCRβ+CD4+CD8α+
TCRβ+CD8αα+
TCRβ+CD8αβ+
Total cells
Vill.Cre-/- Spp-1fl/fl
Vill.Cre+/- Spp-1fl/fl

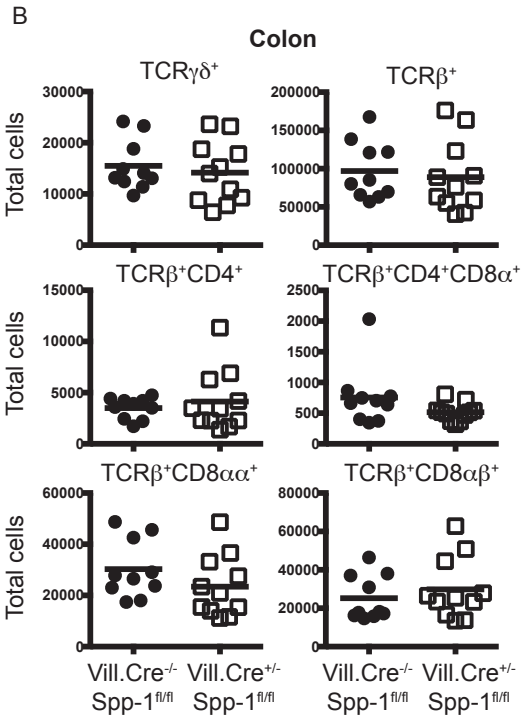
B
Colon
TCRγδ+
TCRβ+
TCRβ+CD4+
TCRβ+CD4+CD8α+
TCRβ+CD8αα+
TCRβ+CD8αβ+
Total cells
Vill.Cre-/- Spp-1fl/fl
Vill.Cre+/- Spp-1fl/fl

Figure 7